RADC-TR-61-217

GEOPHYSICAL INSTITUTE

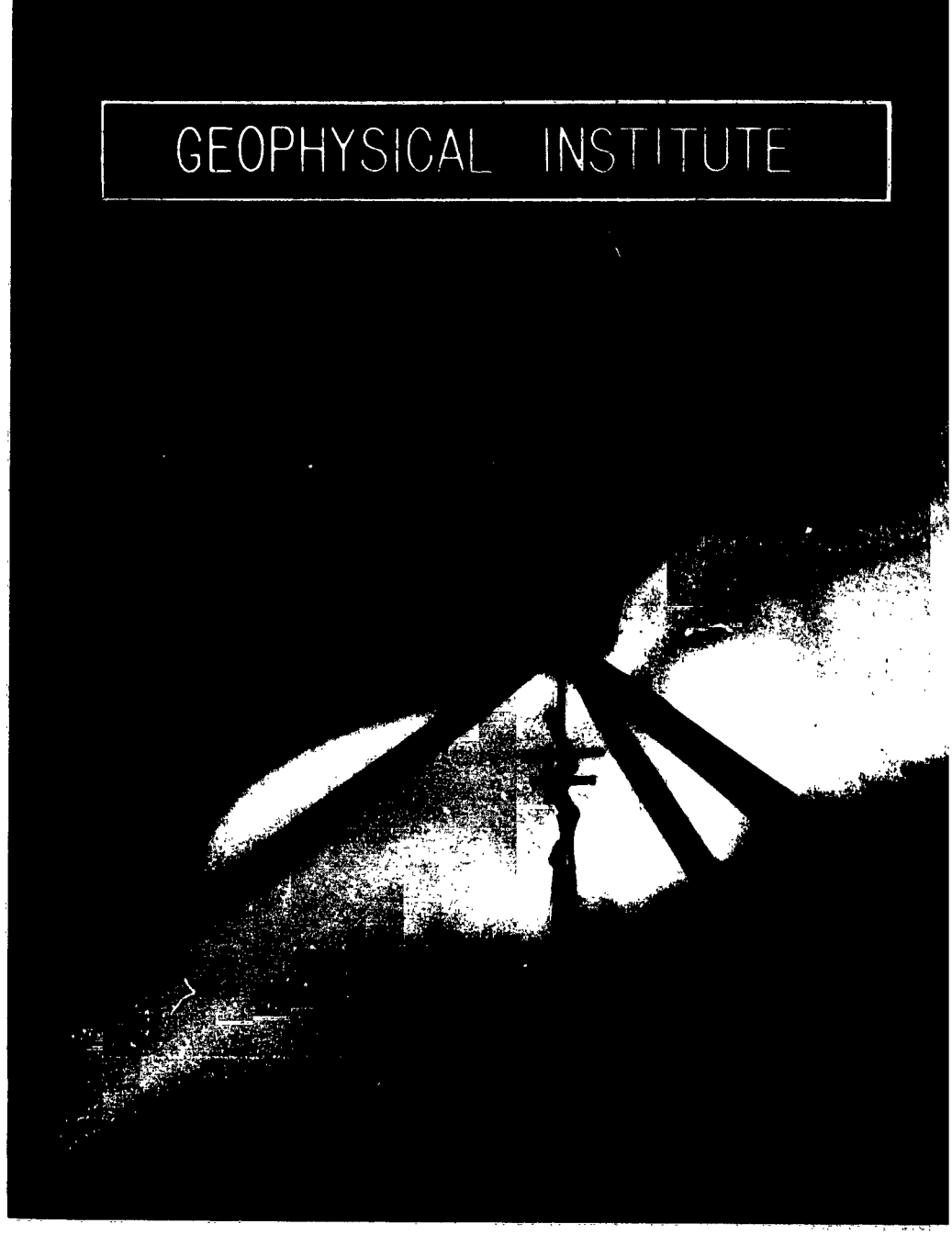

RADIO PROPERTIES OF THE AURORAL IONOSPHERE - PART 1

Final Report

March 1962

Air Force Contract No. AF 30(635)-2887
Project No. 5535 - Task 45774

Rome Air Development Center
Griffiss Air Force Base
Rome, New York

GEOPHYSICAL INSTITUTE

OF THE

UNIVERSITY OF ALASKA

RADIO PROPERTIES OF THE AURORAL IONOSPHERE

Final Report

Air Force Contract No. AF 30(635)-2887

Project No. 5535 - Task 45774

Rome Air Development Center, Griffiss Air Force Base

Rome, New York

March 1962

Report prepared by:

Leif Owren, Editor
C. G. Little
G. H. Reid
R. F. Benson
Z. A. Ansari
R. P. Basler
R. N. DeWitt
W. B. Murcray
J. H. Pope

Report approved by:

V. P. Hessler

V. P. Hessler
Acting Associate Director

FRONTISPIECE

1. The purpose of the contract was to provide experimental data concerning refraction, absorption and scintillation of radio waves propagated through the auroral ionosphere.

2. The contractor's approach to the porblem was to employ standard interferometer techniques to monitor the radiation from radio stars. Much valuable data were obtained and evaluated.

3. The results have extended the state of knowledge of the fine scale structure of the auroral ionosphere and its effects on radio wave propagation. Interferometry techniques were employed to monitor the electronic radiation from "radio stars". Statistical data were collected on the phase and amplitude scintillations of this energy caused by both the "normal" and "disturbed" ionosphere. These data were then examined to determine the dependence between the scintillations and freqeuncy of operation, solar time, zenith angle, and angular size of the radio "source". The data were also correlated with the following known phenomena: Spread F, Sporadic E, magnetic disturbances and auroral activity. Conclusions were then drawn concerning the size, shape and orientation of the small scale irregularities in the auroral ionosphere.

4. The ionosphere has been a field of study for scientists for many years and probably will continue to be for many years to come. This item fits into a vast storehouse of knowledge that man hopefully will someday fill.

5. This specific piece of information is being used as a guide by present systems engineers and also as a guide in the design of future experiments concerning the auroral ionosphere.

TABLE OF CONTENTS - PART 1

TABLE OF CONTENTS - PART 2

II High Latitude Observations of Radio Star Scintillations

by

C. G. Little and G. H. Reid

TABLE OF CONTENTS - PART 3

Page

PREFACE

This presentation constitutes the final report on Contract No. AF 30(635)-2887, Radio Properties of the Auroral Ionosphere. The work carried out under this contract is described in Sections I, II and VI. The results of other programs given in Sections III-V and VII are included because they are considered pertinent. Each section is essentially self-contained. Section I reviews the theory of single scattering of radio waves in weak anisotropic irregularities, extends it to multiple scattering, and explains observed radio star visibility reductions in terms of this process. Section II describes the radio star scintillation observations performed under the contract, and contains an analysis and interpretation of these observations. Subsequent radio star observations during auroral activity are reported in Section III. The relation between spread F and radio star scintillations is discussed in Section IV. Satellite radio signal scintillations are considered in Section V, while Section VI discusses electron density measurements above the F layer peak by means of satellite radio transmissions. Section VII treats high-latitude radio aurora observed on VHF and UHF radars.

The investigators connected with the contract do not agree among themselves on the role which the finite size of the radio stars plays in producing the observed long-duration visibility fades, and two points of view are presented. The difference of opinion appears to reflect divergent evaluations of the physical process involved.

The final report is submitted in three parts due to the amount of material included.

List of Illustrations

List of Tables

I THEORY OF RADIO WAVE SCATTERING IN THE AURORAL IONOSPHERE

by

Leif Owren

1. Introduction

The purpose of Section I is to review those elements of the theory of radio wave scattering and diffraction which have a bearing on the experimental studies reported in Sections II-VII. The review is based mainly on papers by Booker[1,2], Ratcliffe[3], and Fejer[7].

All the experimental evidence obtained at College, Alaska from radio investigations of the E and F layer over the frequency range from 1 to 800 Mc/s indicates that presence of field-aligned, i.e., monisotropic, electron density irregularities is a characteristic property of the auroral ionosphere under quiet as well as disturbed conditions. This makes it particularly important to consider the existing theory for radio scattering and diffraction by nonisotropic irregularities. A basic paper on radio scattering in the troposphere was published by Booker and Gordon[4] in 1950 and extended to nonoisotropic scatterers in the auroral ionosphere by Booker[1] in 1956. A critical examination of the theoretical developments in these two papers show that they contain hidden assumptions which affect ionospheric applications of the theory. Physical factors and some observations which are important for model descriptions of the auroral ionosphere are discussed, and show the need for a theory of multiple forward scattering in thick layers of weak, anisotropic irregularities. This theory is developed and applied to radio star visibility fades observed with interferometers.

2. Scattering by Dielectric Irregularities

Booker and Gordon[4] considered in 1950 the problem of radio wave scattering in a medium of capacitivity, ϵ, containing weak irregularities, i.e., small local fluctuations $\Delta\epsilon$. The suggestive designation "dielectric noise" is sometimes used for such fluctuations (Silverman[5,6]). The physically important quantity is the relative fluctuation or relative deviation $\Delta\epsilon/\epsilon$.

In general the capacitivity is a point function $\epsilon = \epsilon(\underline{r})$, depending on the position $\underline{r}$: (x,y,z) in the medium relative to a fixed frame of reference, O-xyz. Define the local deviation by

$$\Delta\epsilon(x,y,z) = \epsilon - \mathcal{E}\epsilon = \epsilon - \overline{\epsilon} \tag{1}$$

where $\mathcal{E}\epsilon = \overline{\epsilon}$ is the expectation value or mean value of ϵ for the neighborhood of (x,y,z). Thus $\overline{\epsilon}$ is also, in general, a function of position in the medium.

We have

$$\Delta\epsilon/\overline{\epsilon} = (\epsilon-\overline{\epsilon})/\overline{\epsilon} \tag{2a}$$

$$\Delta\epsilon/\epsilon_o = (\epsilon-\overline{\epsilon})/\epsilon_o \tag{2b}$$

where ϵ_o denotes the free space value. Hence

$$\Delta\epsilon/\epsilon_o = (\Delta\epsilon/\overline{\epsilon})\ (\overline{\epsilon}/\epsilon_o). \tag{2c}$$

The elctric field strength at a point Q in the scattering volume v due to linearly polarized radiation from an isotropic transmitter T of power P_T at a large distance R_o (see Fig. I.1) from v is

$$E_Q = \sqrt{(ZP_T/2\pi)}\ \ e^{j(\omega t - kR_o)}/R_o \tag{3}$$

where $\hat{Z}$ is the intrinsic impedance of the medium and k is the propagation constant. The harmonic time factor $\exp(j\omega t)$ will be omitted in the following. A deviation $\Delta\epsilon$ at Q produces a change of

$$\Delta P = \bar{E}\Delta\epsilon \tag{4}$$

in the electric moment per unit volume,

and the contribution from a volume element dv to a receiver at a large distance R from v is

$$d\overline{\Pi}_R = (1/4\pi)\, \bar{E}_Q(\Delta\epsilon/\epsilon_o)\, e^{-jkR}\, dv/R \tag{5}$$

Here the scatter field is expressed in terms of its polarization potential. Hence the total scatter field at R is obtained by integrating over v

$$\overline{\Pi}_R = \int_v d\,\overline{\Pi}_R\, dv \tag{6}$$

Choose a reference point O which may be located on the ground under the scattering volume v, or in this volume itself. Consider two points Q and Q' in the scattering volume inside respectively the scattering volume elements dv and dv' (see Fig. I.1). Denote the different distances as follows:

$$OT = \underline{r}_T \;,\quad OR = \underline{r}_R \;,\quad OQ = \underline{r}^o \;,\quad OQ' = \underline{r}' \;, \tag{7}$$

$$QQ' = \underline{r}$$

$$TQ = \underline{R}_o \;,\quad TQ' = \underline{R}_o' \;,\quad RQ = \underline{R} \;,\quad RQ' = \underline{R}'$$

It will also be convenient to introduce two unit vectors, $\underline{t}$ and $\underline{s}$, in the direction of incidence and scattering respectively:

(8a) $$\underline{t} = (\ell_1, m_1, n_1) = \underline{R}_o/R_o$$

(8b) $$\underline{s} = (\ell_2, m_2, n_2) = -\underline{R}/R$$

(8c) $$\underline{t} \cdot \underline{s} = \ell_1\ell_2 + m_1m_2 + n_1n_2 = \cos\theta$$

Denote the difference vector $\underline{s} - \underline{t}$ by

(8d) $$\underline{d} = \underline{s} - \underline{t}$$

Then the phase difference at R between the waves scattered at Q and Q' is

(8e) $$\Delta\phi = k\underline{r} \cdot (\underline{s} - \underline{t}) = k\underline{r} \cdot \underline{d}$$

Now

(9) $$\overline{\Pi}_R = (1/4\pi)\sqrt{(ZP_T/2\pi)} \int_V (\Delta\epsilon/\epsilon_o) e^{-jk(R_o+R)} dv/R_oR$$

$$= (E_Q/4\pi R) \int_V (\Delta\epsilon/\epsilon_o) e^{-jk(R_o+R)} dv$$

neglecting the variations of R_oR in the magnitudes of the contributions from the different elements dv of v_1 but not in the phases.

The complex power density at R due to scattering in v is

(10) $$\frac{1}{2}EH^* = \frac{1}{2}(Y^*E_Q^2/4\pi R)\, k^2 \sin X \quad |I|^2$$

where

(11) $$|I|^2 = \int_V \int_V \Delta(r^o)\, \Delta(r')^*\, e^{jk\underline{d}\cdot\underline{r}}\, dr^o dr'$$

This result follows from use of the relations:

(12a) $$E = k^2 \Pi \sin X$$

(12b) $$H = YE = E/Z$$

where X is the angle between the direction of scattering $\underline{s}$ and the direction of the incident E field vector, and

$$\underline{R}_o - \underline{R}'_o = -\underline{r} \ , \ R - R' = \underline{r} \tag{13a}$$

$$\underline{t} \cdot \underline{r} = \ell_1 x' + m_1 y' + n_1 z' \tag{13b}$$

$$-\underline{s} \cdot \underline{r} = \ell_2 x' + m_2 y' + n_2 z' \tag{13c}$$

with the abbreviations

$$\Delta(r^o) = \Delta\epsilon/\epsilon_o(x,y,z) \tag{14a}$$

$$\Delta(r') = \Delta(r^o+r) = \Delta\epsilon/\epsilon_o(x',y',z') \tag{14b}$$

$$dr^o = dxdydz \quad , \quad dr' = dx'dy'dz' \tag{14c}$$

If T and R are at great distances from v, and the linear dimensions of v small compared with R_o and R, then $\underline{R}_o$ and $\underline{R}'_o$ are practically parallel.

Let C(r) denote the autocovariance function

$$C(r) = \int_v \Delta(r^o)\ \Delta(r^o+r)^*\ dr^o \tag{15}$$

and

$$C(0) = \int_v \left|\Delta(r^o)\right|^2 dr^o \tag{16}$$

Then we may define a normalized autocovariance or an <u>auto-correlation function</u>

$$R(r) = C(r)/v\ C(o) \tag{17}$$

and write for (11)

$$|I|^2 = v\ C(o) \int_v R(r)\ e^{jk\underline{d}\cdot\underline{r}}\ dr \tag{18}$$

since $dr' = d(r^o+r) = dr$.

We have now reached a crucial point in the Booker-Gordon analysis, and it is desirable to reiterate the essential assumptions introduced so far. These are:

Ass. 1 The distances OQ, OQ' and RQ, RQ' are large compared with the linear dimensions of the scattering volume.

Ass. 2 The scatter field is weak compared with the incident field (Born approximation - the scatter field represents a second order effect. This requires that $\Delta\epsilon/\epsilon_o$ be small.

$$\Delta\epsilon/\epsilon_o \ll 1$$

We must now introduce two more assumptions in order to follow the Booker-Gordon theory.

Ass. 3 The mean, local capacitivity $\bar{\epsilon}$ differs insignificantly from ϵ_o in the scattering volume:

$$\bar{\epsilon} \simeq \epsilon_o \qquad \text{in } v$$

so, to the first order,

$$\Delta\epsilon/\epsilon_o\ (x,y,z) = \Delta\epsilon/\bar{\epsilon}\ (x,y,z).$$

Having made this assumption we can drop the subscript from ϵ_o and the bar from $\bar{\epsilon}$ in the following.

The fourth assumption is less obvious and of the greatest importance. Let the relative deviation $\Delta = \Delta\epsilon/\epsilon$ represent a random process with the probability density function f(u) where $u = |\Delta\epsilon/\epsilon|$. Then the variance or mean square fractional deviation is

$$\text{Var}(u) = \overline{|\Delta\epsilon/\epsilon|^2} = \int_{-\infty}^{+\infty} u^2 f(u)\,du. \tag{19}$$

if the integral converges.

Now provided the random process is ergodic, which in practice implies a stationary gaussian process with zero mean, the variance is also given by

$$\text{Var}(u) = \lim_{V \to \infty} \frac{1}{V} \int_V u^2 \, dv \tag{20}$$

but not otherwise. Therefore we are forced to make one further assumption:

Ass. 4 The relative deviations $\Delta\epsilon/\epsilon$ represent a gaussian random process with zero mean which is spatially stationary.

This implies that the random variable $u = |\Delta\epsilon/\epsilon|$ must have a probability density function of form

$$f(u) = \sqrt{(1/2\pi u_o^2)} \quad e^{-(u/u_o)^2/2}$$

and that this function may not depend on the space point (x,y,z) in the scattering volume. That is, the process must be statistically uniform in space. Under this condition we can write for (16)

$$C(0) = \overline{|\Delta\epsilon/\epsilon|^2} \tag{21}$$

and for (18)

$$|I|^2 = v \, \overline{|\Delta\epsilon/\epsilon|^2} \int R(r) e^{jk\underline{d}\cdot\underline{r}} \, dr \tag{22}$$

For a stationary gaussian process the Wiener-Khintchin theorem may be invoked. This theorem states that for a zero-mean stationary process $u(t)$, the power spectral density $G(\omega)$ and the autocorrelation function $R(T)$ of $u(t)$ are Fourier transform mates:

$$G(\omega) = \int_{-\infty}^{+\infty} R(T) \, e^{-j\omega T} \, dT \tag{23a}$$

(23b) $$R(\tau) = \int_{-\infty}^{+\infty} G(\omega)\, e^{j\omega t}\, d\omega/2\pi$$

provided $G(\omega)$ is absolutely continuous (the physical case) and non-negative.

Therefore we have, under assumption 4,

(24) $$|I|^2 = v\, \overline{|\Delta\epsilon/\epsilon|^2}\, P(\theta)$$

where $P(\theta)$ denotes $P\left[k(\ell_2-\ell_1),\ k(m_2-m_1),\ k(n_2-n_1)\right]$, and

(25a) $$P(\theta) = \int_{-\infty}^{+\infty} R(r)\, e^{jk\underline{d}\cdot\underline{r}}\, dr$$

(25b) $$R(r) = \int_{-\infty}^{+\infty} \Delta(r^o)\Delta(r^o+r)^*\, dr^o \Big/ \int_{-\infty}^{+\infty} |\Delta(r^o)|^2\, dr^o$$

The power scattering cross-section (power scattered per unit solid angle, per unit incident power density, per unit volume) is therefore:

(26a) $$\sigma = (1/v)\, \left[R^2|E|^2/2Z\right] / \left[P_T/4\pi R_o^2\right]$$

or

(26b) $$\sigma = (1/v)\, \pi^2 \sin^2 X\, |I|^2/\lambda^4$$

or

(26c) $$\sigma = \overline{|\Delta\epsilon/\epsilon|^2}\, (\pi^2 \sin^2 X/\lambda^4)\, P(\theta)$$

The direction $\underline{d} = \underline{s} - \underline{t}$ is the external bisector of the angle θ between the direction of incidence and the direction of scattering. The vector $\underline{d}$ is normal to the plane which mirrors the incident wave into the direction of scatter and defines what is known as the mirror direction. The mirror plane is therefore

defined by the vector equation

(27) $\underline{R} \cdot \underline{d} = p \quad , \quad p =$ distance from R

This mirror plane may be regarded as an "aperture" plane for the scattered radiation. A corrugation along the "aperture" plane of wave length

(28) $/_{\perp} = \lambda/2 \sin(\theta_o/2)$

will produce constructive interference of wavelets in the direction of scatter θ_o.

3. Ionospheric Single Scattering by Anisotropic Irregularities

Two more steps are required to obtain formulas useful for the ionosphere:

(a) A specific autocorrelation function R(r) must be selected.

(b) The variance of $|\Delta\epsilon/\epsilon|$ must be expressed in terms of the ionospheric electron density N or refractive index $n = \mu - j\chi$.

3.1 Autocorrelation Functions.

The following forms for the autocorrelation function have been introduced by various authors:

Booker-Gordon[4]

(29) $$R(r) = \exp\{-r/L\}$$

Fejer[7]

(30) $$R(r) = \exp\{-(r/L)^2\}$$

Booker[1]

(31a) $$R(x,y,z) = \exp\left\{-\frac{1}{2}\left[(x/a)^2 + (y/b)^2 + (z/c)^2\right]\right\}$$

(31b) $$R(x,y,z) = \exp\left\{-\frac{1}{2}\left[(x^2+y^2)/T^2 + z^2/L^2\right]\right\}$$

Renau[8]

(32a) $$R(x,y,z) = \exp\left\{-\sqrt{\left[(x/a)^2 + (y/b)^2 + (z/c)^2\right]}\right\}$$

(32b) $$R(x,y,z) = \exp\left\{-\sqrt{((x^2+y^2)/T^2 + z^2/L^2)}\right\}$$

The resulting expressions for $P(\theta)$ are

(29') $$P(\theta) = \frac{8\pi L^3}{\left[1 + (2kL)^2\sin^2(\theta/2)\right]^2}$$

(30') $$P(\theta) = \pi^{3/2} L^3 \exp\left\{-k^2L^2\sin^2(\theta/2)\right\}$$

(31a') $$P(\ell,m,n) = (2\pi)^{3/2}\, abc\, \exp\left\{-\frac{1}{2}k^2\left[a^2(\ell_2-\ell_1)^2+b^2(m_2-m_1)^2+c^2(n_2-n_1)^2\right]\right\}$$

(31b') $$P(\theta,n) = (2\pi)^{3/2}\, T^2\, L\, \exp\left\{-2k^2T^2\sin^2(\theta/2)\right\}\exp\left\{-\frac{1}{2}k^2(L^2-T^2)n^2\right\}$$

where $n^2 = (n_2-n_1)^2$

(32a') $$P(\ell,m,n) = \frac{8\pi\, abc}{\left\{1 + k^2\left[a^2(\ell_2-\ell_1)^2 + b^2(m_2-m_1)^2 + c^2(n_2-n_1)^2\right]\right\}^2}$$

(32b') $$P(\theta,n) = \frac{8\pi LT^2}{\left\{1 + k^2\left[2T^2\sin^2\theta/2 + (L^2-T^2)(n_2-n_1)^2\right]\right\}^2}$$

The derivation of the expressions (29') through (31') is elementary, and follows Fejer's[7] method for (32a') and (32b'). The choice of the autocorrelation function from physical consideration is discussed in Subsection 4.

3.2 Ionospheric Expressions for the Variance of $|\Delta\epsilon/\epsilon|$.

The capacitivity of the ionosphere neglecting collisions and the magnetic field is

$$\epsilon/\epsilon_o = 1 - \omega_N^2/\omega^2 \tag{33}$$

where

$$\omega_N^2 = (e^2/\epsilon_o m)\, N$$

N = electron density, e = electronic charge, m = electron mass, in rationalized MKS-units.

Hence

$$\begin{aligned} \Delta\epsilon/\epsilon &= -(\epsilon_o/\epsilon)\, \Delta\omega_N^2/\omega^2 \\ &= -(k_o/k)^2\, \Delta\omega_N^2/\omega^2 \\ &= -(\lambda/\lambda_o)^2\, \Delta\omega_N^2/\omega^2 \end{aligned} \tag{34}$$

and

$$\begin{aligned} |\Delta\epsilon/\epsilon| &= (\lambda/\lambda_o)^2\, |\Delta\omega_N^2/\omega^2| \\ &= (\lambda/\lambda_o)^2\, (\omega_N/\omega)^2\, |\Delta N/N| \end{aligned} \tag{35}$$

$$|\Delta\epsilon/\epsilon|^2 = (\lambda/\lambda_o)^4\, (\omega_N/\omega)^4\, |\Delta N/N|^2 \tag{36}$$

If, as before, $|\Delta\epsilon/\epsilon|$ represents a spatially stationary gaussian process and further if also:

Ass. 5 $\quad \omega_N^2 = (e^2/m\epsilon_o)N(x,y,z)$ is constant,

that is, $N(x,y,z) = N$ = constant

then, and only then, can we set

$$\overline{|\Delta\epsilon/\epsilon|^2} = (\lambda/\lambda_N)^4\, \overline{|\Delta N/N|^2} \tag{37}$$

using $\omega_N/\omega = \lambda/\lambda_N$ and assumption 3

$$\lambda/\lambda_N = \lambda_o/\lambda_N$$

The cross-section for scattering of UHF or sufficiently high VHF radio waves by weak irregularities in the ionosphere then reads

$$(38) \qquad \bar{\sigma}(\theta,X) = \overline{\left|\Delta N/N\right|^2} \left(\pi \sin X/\lambda_N^2\right)^2 P(\theta)$$

where λ_N is the plasma wavelength corresponding to the electron density N.

Sometimes it is convenient to express $\overline{\left|\Delta\epsilon/\epsilon\right|^2}$ in terms of the relative fluctuation in the refractive index $\Delta\mu/\mu$ rather than $\Delta N/N$. We have

$$(39a) \qquad \epsilon/\epsilon_o = \mu^2$$

$$(39b) \qquad \Delta\epsilon/\epsilon_o = 2\mu\Delta\mu + (\Delta\mu)^2$$

$$(39c) \qquad \Delta\epsilon/\epsilon = 2(\Delta\mu/\mu) + (\Delta\mu/\mu)^2$$

Let $x = \Delta\epsilon/\epsilon$, $t = \Delta\mu/\mu$ so

$$(40b) \qquad t = \sqrt{(1+x)} - 1$$

Now, if x is a random variable with the density function f(x) and t is a strictly increasing, or strictly decreasing, function of x, then t is a random variable with the density function

$$(41) \qquad g(t) = f\left[x(t)\right] \; x'(t)$$

where x(t) is the inverse function to t(x).

Therefore, setting

$$(42a) \qquad f(x) = \sqrt{(1/2\pi x_o^2)} \exp\left\{-\tfrac{1}{2}\,(x/x_o)^2\right\}$$

so

$$\overline{x^2} = \int_{-\infty}^{+\infty} x^2 f(x)dx = x_o^2 \tag{42b}$$

it follows that

$$g(t) = \sqrt{(1/2\pi x_o^2)}\ 2(t+1)\ \exp\left\{-\tfrac{1}{2}(t/x_o)^2\left[t+2\right]^2\right\} \tag{43a}$$

and

$$\overline{t^2} = \sqrt{(1/2\pi x_o^2)} \int_{-\infty}^{+\infty} \left[t^3+t^2\right] \exp\left\{-\tfrac{1}{2}(t/x_o)^2\left[t+2\right]^2\right\} dt \tag{43b}$$

Actually, the limits in the integrals (42b) and (43b) should be finite and not infinite because of the assumption

$$\left|x\right| = \left|\Delta\epsilon/\epsilon\right| \ll 1$$

so we shall take the integral (42b) over the interval (-a,a) and the integral (43b) over the corresponding interval (-b,b)

Then,

$$\overline{x^2} = x_o^2\ \mathrm{erf}(a/x_o\sqrt{2}) - \sqrt{(2/x_o)}\ ax_o\ \exp\left\{-\tfrac{1}{2}(a/x_o)^2\right\} \tag{44}$$

Consider the integral (43b). If the variance of x

$$\overline{x^2} \simeq x_o^2$$

is very small, the main contribution to t^2 in (43b) will come from values of t which are much smaller than unity. Therefore, if we neglect t compared with 2 in the expontential factor $\left[t+2\right]^2$ we obtain

$$t^2 \approx (2/x_o)\sqrt{(2\pi)} \int_{-b}^{b} \left(t^3+t^2\right) e^{-2(t/x_o)^2}\ dt \tag{45}$$

The first of the two resulting integrals vanishes, and we find

$$\overline{t^2} = (x_o^2/4)\ \mathrm{erf}(b\sqrt{2}/x_o) - \sqrt{(2/\pi)}\ (bx_o/2)\ e^{-2(b/x_o)^2} \tag{46}$$

Therefore,

$$(47)\qquad \overline{(\Delta\epsilon/\epsilon)^2} = x_o^2 \left[\operatorname{erf}(a/x_o\sqrt{2}) - (2a/\pi x_o)\exp -\tfrac{1}{2}(a/x_o)^2\right]$$

$$(48)\qquad \overline{(\Delta\mu/\mu)^2} = \frac{x_o^2}{4}\left[\operatorname{erf}(a/x_o\sqrt{2}) - \sqrt{(a/2\pi x_o)}\exp -\tfrac{1}{2}(a/x_o)^2\right]$$

Now, provided

$$(49a)\qquad \left|\Delta\epsilon/\epsilon\right| \leq 1/10 \qquad \text{or}$$

$$(49b)\qquad \left|\Delta\mu/\mu\right| \leq 1/20 \qquad \text{and}$$

$$(49c)\qquad x_o \leq 2 \times 10^{-2}, \quad x_o \leq 0.2\left|\Delta\epsilon/\epsilon\right|_{max}$$

$$(49d)\qquad x_o^2 \leq 4 \times 10^{-4}, \quad (\Delta\epsilon/\epsilon)^2 \leq 4 \times 10^{-4}$$

it is readily seen that equation (48) reduces to

$$(50)\qquad \overline{(\Delta\mu/\mu)^2} = \tfrac{1}{4}\,\overline{(\Delta\epsilon/\epsilon)^2}$$

Therefore, under these conditions together with the assumptions 1-5 made earlier,

$$(51)\qquad \sigma(\theta,X)\ \overline{\left|\Delta\mu/\mu\right|^2}\ (2\pi \sin X/\lambda^2)^2\ P(\theta)$$

When collisions are neglected so the quantities $\Delta\epsilon/\epsilon$ and $\Delta\mu/\mu$ are real, it makes no difference whether we use absolute value signs or parantheses for the squared quantities in the equations. We have used this fact freely above.

4. Physical Considerations

The autocorrelation function (29), $R(r) = \exp - (r/L)$, gives a good empirical description of the irregularities associated with isotropic turbulence (Pekeris[9]). It was therefore used in the Booker-Gordon theory of tropospheric radio scattering and also applied to ionospheric scattering by Bailey et al[10]. It will be seen that this particular form of the autocorrelation function implies a scattering medium having irregularities with sharp points or discontinuities in the electron density distribution. This was thought to be an unrealistic assumption for ionospheric scattering, and Fejer[7] therefore used instead the functional form (30), $R(r) = \exp -(r/L)^2$, which also implies a medium with spherical irregularities but having smooth electron density profiles.

It was realized later from radio star scintillation observations (Spencer[11]), that the irregularities in the ionosphere are elongated along the magnetic field lines. Booker[1] then introduced the gaussian autocorrelation function,

(31b) $R(x,y,z) = \exp - \frac{1}{2}\left[(x^2+y^2)/T^2 + z^2/L^2\right]$, in connection with his theory for VHF backscatter from auroral columns of ionization. Later Renau[8] used the function,

(32b) $R(x,y,z) = \exp - \sqrt{\left[(x^2+y^2)/T^2 + z^2/L^2\right]}$, for a theory of spread F. Comparison of the corresponding expressions for $P(\theta)$, equations (31b') and (32b'), with equations (29') and (30'), shows that the modification in going from Booker's model to Renau's in an ionosphere with anisotropic irregularities corresponds closely

to that of going from Fejer's model to the Booker-Gordon description in an ionosphere with isotropic irregularities.

The discussion by Booker and Gordon[4] of scattering in a medium with spherical irregularities brings out some important points which have validity also for other shapes of electron density profiles. Thus their discussion implies that in a medium containing both large and small irregularities, the forward scatter depends on the large irregularities while the small irregularities control the backscatter. For isotropic (spherical) scatterers the equation (38) together with (29') or (30') show that in the case of forward scatter, ($\theta = 0$),

$$(52) \qquad \sigma_F \propto (kL)^3$$

regardless of the scale size, L, and for both of the profiles $R(r) = \exp - (r/L)$ and $\exp -(r/L)^2$. For backscatter, ($\theta = \pi$), we have similarly

$$(53) \qquad \sigma_B \propto (kL)^3 \qquad \text{when} \qquad kL \ll 1$$

but

$$(54a) \qquad \sigma_B \propto (kL)^{-1} \qquad \text{for} \qquad R = e^{-(r/L)}$$

$$(54b) \qquad \sigma_B \propto (kL)^3 \, e^{-(kL)^2} \qquad \text{for} \qquad R = e^{-(r/L)^2}$$

when $kL \gg 1$.

The formulas (29') and (30') show that when the scale size is much larger than wavelength, $kL \gg 1$, the scatter is mainly forward and confined to a cone with half-power beamwidth, $2\theta_b$, about the direction of incidence, $\theta = 0$, which is

(55a) $2\theta_b = 1.3/kL$ for $R = e^{-(r/L)}$

(55b) $2\theta_b = 3.3/kL$ for $R = e^{-(r/L)^2}$

For forward scatter and backscatter the two profiles therefore lead to different results only when the scale of irregularities is larger than the wavelength of the incident radiation, $L >> \lambda/2\pi$. The profile exp - (r/L) gives a slightly narrower forward scatter cone than exp $-(r/L)^2$, and backscatters a larger fraction of the incident radiation.

Another important point made by Booker and Gordon is that the power polar diagram of scattering for a medium containing a statistical distribution of irregularity sizes is the same as the amplitude polar diagram of a single irregularity whose cross-sectional profile of $\Delta\epsilon$ is proportional to the autocorrelation function, R, for $\Delta\epsilon$. This means that in the case of forward scattering, for $kL >> 1$, we can infer what the scattering power polar diagram will be by regarding the cross-section of a single irregularity as the aperture plane of an antenna. In other words, the usual antenna formulas connecting beamwidth and aperture width apply, only the angular spectrum or polar diagram is the power spectrum rather than the amplitude spectrum because the Fourier transform of an autocorrelation function rather than of an aperture field distribution is involved. The differences between the scatter polar diagrams for the profiles exp $-(r/L)$ and exp $-(r/L)^2$ when $kL >> 1$ are now readily understandable qualitatively. Although neither of the two autocorrelation functions vanish for finite values of r, the function exp $-(r/L)$ decreases

more slowly for increasing argument than $\exp -(r/L)^2$ after the cross-over at $r = L$ where both functions equal $1/e$. Therefore the profile $\exp -(r/L)$ gives a larger effective aperture width and narrower forward scatter cone than the profile $\exp -(r/L)^2$. The backscatter properties are on the other hand determined by the behavior of the autocorrelation function for small values of the argument, that is, the small scale structure in the irregularities is important. Therefore the sharp peak of $\exp -(r/L)$ at $r = 0$ gives more backscatter than the rounded peak of $\exp -(r/L)^2$.

The observational evidence shows that for the ionosphere in general, and the auroral ionosphere in particular, the electron density irregularities are elongated in the direction of the magnetic field lines and may be described by smooth spheroids of the type

$$(31b) \qquad R(x,y,z) = \exp -\frac{1}{2}\left[(x^2+y^2)/T^2 + z^2/L^2\right]$$

with $L > T$, in a coordinate system where z is parallel to the direction of the geomagnetic field lines. Under disturbed, auroral conditions we may expect sharp local increases or discontinuities of ionization to appear in the general structure of field-aligned irregularities. These local properties may more adequately be described by an autocorrelation function of the form

$$(32b) \quad R(x,y,z) = \exp -\sqrt{\left[(x^2+y^2)/T_1^2 + z^2/L_1^2\right]}, \text{ with } T_1 \leq T \text{ and } L_1 \leq L.$$

This suggests that the appropriate model for the aurorally disturbed ionosphere might be a statistical collection of smooth field-aligned irregularities, such as described by the

autocorrelation function (31b), with sharp cores as described by the function (32b). Thus a description in terms of two sets of simultaneously occurring irregularities is proposed, involving a combination of larger, smooth ellipsoids according to formula (31b) and smaller, sharp irregularities characterized by formula (32b) where the values of the parameters T and L may be different. Since forward scatter is controlled by the large irregularities and backscatter by the small, this indicates that the scattering law should be taken as (31b') for forward scatter but possibly as (32b') for backscatter under disturbed conditions. For quiet or normal conditions the autocorrelation function(31b) and the law of scattering (31b') may probably be used both for forward scatter and backscatter.

In both cases the appropriateness of the model must be decided on an empirical basis from the observed properties of radio signals from radio stars and artificial satellites traversing the auroral ionosphere as well as from radar backscatter in auroral ionization.

The properties of the forward scatter polar diagram for the scattering law (31b') may be inferred from the fact that the cross-section of the $\Delta\epsilon$ surface, $\Delta\epsilon(x,y,z)$ = constant, in the plane having the direction of incidence as its normal is in general an ellipse. The scatter beam must accordingly have an elliptical cross-section. The minor axis of this ellipse lies in the plane through the z-axis and the direction of incidence, perpendicular to the latter, and the major axis is parallel to the xy-plane. The major axis is the same for all directions of incidence, and the half-power beamwidth in this direction is

$2\theta_b = 2.4/kT$ for the law (31b'). The minor axis length depends on the angle between the z-axis and the direction of incidence. For directions of incidence parallel to the field lines the scatter beam is circular and has the half-power beamwidth just stated. We shall confirm these deductions by a discussion of the formula (31b') in the next sub-section. It may be noted that for nearly vertically elongated irregularities as in the auroral zone, the wide dimension of the scatter beam cross-section is nearly horizontal.

Intermediate latitude observations of radio star scintillations have indicated that the region producing the scintillations is somewhere in the upper F layer, possibly at a height of about 400 km (Hewish[12]). Investigations of the scintillations in radio signals from artificial satellites made in the auroral zone at Tromsø, as well as at Kjeller, Norway, have recently been reported by Frihagen and Trøim[13]. The observations were made on the frequencies of 20, 40 and 108 Mc/s and show that the height of the causative region is between 300 and 600 km with a mean height of 450 km for the Tromsø observations. The irregularities were found to be highly elongated along the magnetic lines, with a typical width of about 0.6 km for the field-aligned cylinders. The horizontal extent of the patches of irregularities is said to be at least of the order of 1000 km, which agrees with the results of the oblique HF backscatter soundings from College, Alaska (Bates[14]). The authors also note one case of 20 Mc/s scintillations produced by sporadic E irregularities at a height of 104 km. Recent, spaced receiver observations of 20 and 40 Mc/s

satellite radiations at College, Alaska, indicate that E layer induced scintillations may occur more frequently than indicated by the observations in Norway, and typically under disturbed conditions when aurora is present.

Nichols[15] has found evidence of multiple scatter in radio star scintillation observations made at Ithaca, New York, with radio interferometers for 53 and 201.5 Mc/s having antenna pairs spaced about 280 meters (50 wavelengths at 53 Mc/s) apart on East-West and North-South lines. During lower transits of the radio star Cassiopeia A the interference pattern amplitude showed large decreases on 53 Mc/s but only slight decreases on 201.5 Mc/s. The visibility of the 53 Mc/s pattern increased as the antenna spacing was decreased, and the normal amplitude was regained for small spacings of about five wavelengths. The elevation angle of Cas A is 11 degrees during lower transit in latitude 42.5°N which means that the direction of incidence is nearly normal on the magnetic field lines. The geomagnetic latitude of Ithaca, New York is 53.5 degrees so at lower transit the line-of-sight to the radio star crosses the 400 km height level in the auroral zone at geomagnetic latitude 65°N. This is nearly the geomagnetic latitude of College, Alaska (64.5°N).

Visibility reductions or losses similar to those reported by Nichols have been observed at College, Alaska on 223 and 456 Mc/s near upper and lower transit of Cassiopeia A and Cygnus A, as well as at other times, with an East-West tracking interferometer as discussed in Section II.5. The antenna spacing is 68 wavelengths at 223 Mc/s and thus comparable with the 50 wavelengths

spacing for the Ithaca 53 Mc/s interferometer. The visibility fades are deeper at College since in most cases only weak fades occur on 201.5 Mc/s at Ithaca with an antenna spacing of 190 wavelengths. The ionospheric conditions under which the visibility fades of Cas A occur differ in two respects for the two stations: (i) For Ithaca the pathlength through the diffracting region of the auroral F layer is longer than for College by a secant factor, and (ii) At College the line-of-sight to the radio star passes through the auroral E layer which happens only exceptionally for Ithaca. The difference in the angle of incidence on the magnetic field lines has no bearing on the visibility fades because it is the azimuthal scatter beam produced by the transverse irregularity dimension which is important for the near-transit interferometer observations in both cases.

Woodman[16] has reported frequent occurrence of a similar phenomenon in the 108 Mc/s satellite radio signal recordings at the NASA Minitrack stations located near the geomagnetic equator, in Ancon (Peru), Antofagasta (Chile), and Quito (Ecuador). Phase anomalies are observed on the socalled "Fine" East-West interferometer channel which records the phase difference between two antennas spaced 55 wavelengths apart in this direction. The anomaly consists in a distortion of the phase record which in severe cases makes it impossible to reduce. During severe distortions the recorder trace has an irregular, noise-like appearance indicating that no phase correlation exists between the signals from the two antenna. The rapid phase fluctuations are of the order of 360 degrees and correspond to an apparent East-

West movement of the satellite, that is, angular scintillation, of the order of one degree of arc. These anomalies are not observed on the North-South fine channel for which the antennas have the same 55 wavelengths spacing, but phase changes of up to 0.02 wavelengths are evident when the signal disappears on the East-West fine channel. The coarse East-West (narrow antenna spacing) and the fine and coarse North-South channels exhibit correlated, rapid phase fluctuations during the phase anomalies. At Antofagasta sudden transitions from normal to completely irregular phase variations are observed on the wide East-West antenna spacing.

The phase anomalies occur only during the night hours and are most pronounced near midnight. A nearly 100 per cent correlation has been established between the occurrence of phase anomalies and spread F at Ancon while there is a negative correlation with magnetic disturbances as generally observed for equatorial spread F.

Cohen and Bowles[17] have deduced from 50 Mc/s forward scatter studies over South-American transequatorial paths that the scatter in the equatorial F layer occurs in relatively thin sheets or patches about 50 km thick containing field-aligned irregularities. The scattering layer is generally near or below the bottom of the F layer but may occur up to heights of 450 km or more. The field-aligned irregularities are found to have a width of 10 meters or less, and a length in the direction of the field lines of 1 km or more. The above investigation as well as other by Bowles et al[18] and by Egan[19] show that the equatorial

E region is also an important source of VHF scatter. The E region irregularities are field-aligned and appear to be associated with the equatorial electrojet. The scatter echoes have a striking resemblance to VHF echoes from auroral E region ionization. Although the equatorial E layer forward scatter occurs predominantly during the daytime hours, it is also regularly present during the night.

These various observations indicate that under auroral conditions we may expect to have two separate regions of scattering irregularities, located respectively in the upper F layer and the E layer, which contribute to radio star and satellite scintillations. The F layer region probably has considerable depth, making it necessary to allow for multiple scattering. The E layer region may be thin measured in units of length but its scattering properties could nevertheless be such that multiple scattering occurs as we shall see later. The existence of two scattering layers per se requires an extension of the theory for forward scattering in anisotropic irregularities to include the effects of rescatter even if the individual layers may be regarded as thin and singly scattering. A technique for dealing with such multiple scatter conditions is discussed in subsection 6.

It is known from meteor observations that the lower E layer is turbulent. The "Smokepuff" experiments in Florida by Gallagher et al[20] further indicate that the turbulent part of the E layer extends up to heights of about 105 km, but not above, and that there is a sharply defined transition region. In this connection it is of interest to note that statistically the majority of auroral forms observed in the auroral zone have their

lower limits at a similar height (Harang[21]). Størmer[22] has found from a large material on height observations of various auroral forms that the mean height of the lower border of homogeneous arcs is 107 km. Although auroral luminosity is frequently observed below this height down to 80 km, and on rare occasions the lower border of intense rayed arcs and bands may penetrate down to 70 km, the auroral height statistics nevertheless seems to indicate a change in the E layer properties somewhere between 105 and 110 km. Howells[23] has shown that ionization irregularities which are elongated along the magnetic field lines cannot be formed by diffusion processes in the presence of turbulence. In a turbulent, ionized medium with a vertical magnetic field, pancake-shaped irregularities elongated in the horizontal direction will form. The implication of this is that the large scale electron density profiles in the lower E layer and the D layer may be described by autocorrelation functions of the form (31b) with $T \gg L$ rather than the usual assumption of $T \ll L$ or $T < L$ used for the upper E layer and the F layer. The small scale irregularities formed under auroral conditions by particle radiation incident parallel to the magnetic field lines would probably still be described by the autocorrelation function (32b) with $T_1 < L_1$ even in the lower E layer. These special conditions should be kept in mind when high latitude observations of scatter from electron density irregularities known or believed to occur below about 105 km are interpreted.

It should be noted that the correlation or scale lengths T and L appearing in the equations for the scattering cross-sections

are not the actual physical lengths of the scattering irregularities, but differ from these by a numerical factor. The value of this factor depends on the particular form of the autocorrelation function. Rice[24] has shown that if a random function, $f(x)$, has the autocorrelation function, $R(x)$, then the average distance, d, between the maxima of $f(x)$ is

$$(56) \qquad (d/2\pi)^2 = -R_o'' / R_o^{(4)}$$

This gives for

$$(57a) \qquad R(x) = e^{-(x/x_o)} \quad , \quad d = 2\pi x_o = 6.3x_o$$

$$(57b) \qquad R(x) = e^{-(x/x_o)^2} \quad , \quad d = 2\pi x_o/\sqrt{6} = 2.6x_o$$

$$(57c) \qquad R(x) = e^{-\frac{1}{2}(x/x_o)^2} \quad , \quad d = 2\pi x_o/\sqrt{3} = 3.6x_o$$

A last physical point of some importance is the magnitude of the relative mean square deviation of electron density, $\overline{(\Delta N/N)^2}$, which appears in the equation (38) for the scattering cross-section. Booker[1] has deduced a value of

$$(58a) \qquad \overline{(\Delta N/N)^2} = 3 \times 10^{-7}$$

on the assumption that a suitable estimate for the plasma wavelength is $\lambda_N = 30$ m, corresponding to a critical frequency of 10 Mc/s for auroral E layer ionization. This value has been corrected by Nichols[25] to

$$(58b) \qquad \overline{(\Delta N/N)^2} = 6 \times 10^{-4}$$

based on auroral backscatter studies on 41 and 106 Mc/s at College, Alaska, and a change of plasma wavelength to the more reasonable value of $\lambda_N = 50$ m corresponding to a critical frequency of 6 Mc/s. If Booker's premises are accepted otherwise but the plasma wavelength increased to 50 meters, the value

$$\overline{(\Delta N/N)^2} = 2.5 \times 10^{-6} \tag{58c}$$

results. Thus the mean square value of $\Delta N/N$ appears to be in the range 10^{-4} - 10^{-6}.

5. Angular Power Spectrum After Single Scattering

The previous considerations show that the law of scattering is

$$\sigma = \overline{|\Delta N/N|^2} \; (\pi \sin X/\lambda_N^2)^2 \; P(\theta,n) \tag{59}$$

with

$$P(\theta,n) = (2\pi)^{3/2} \, T^2 L \, e^{-2k^2T^2\sin^2\theta/2} \, e^{-\frac{1}{2}k^2(L^2-T^2)n^2} \tag{60a}$$

or

$$P(\theta,n) = \frac{8\pi T^2 L}{\left[1 + k^2(2T^2\sin^2\theta/2 + (L^2-T^2)n^2)\right]^2} \tag{60b}$$

and

$$n^2 = (n_2 - n_1)^2 \tag{60c}$$

Eqn. (59) with (60a) will be used for forward scatter under all conditions and possibly should be used to describe backscatter under normal conditions, but (59) with (60b) is more likely to apply for backscatter under disturbed conditions.

The experimental evidence indicates that the scale lengths T and L for the large irregularities which control the forward scatter are one or two orders of magnitude larger than any radio wavelength used in VHF investigations. The scale lengths deduced from VHF and UHF backscatter observations of auroral E layer ionization are much smaller, and generally a value for T of the order of the exploring radio wavelength is found.

Some properties of the angular power spectrum and the scatter beam can be inferred from the expressions for $P(\theta,n)$. Let the direction cosines (l, m, n) be expressed in terms of the angles (α, β, γ) by

$$l = \cos\alpha, \qquad m = \cos\beta, \qquad n = \cos\gamma \tag{61}$$

As before the direction cosines for the incident wave are denoted by (l_1, m_1, n_1) and the direction cosines for the scattered wave by (l_2, m_2, n_2). The direction cosines (l, m) and the corresponding angles (α,β) have disappeared from the expressions for $P(\theta,n)$ through use of the identities

$$l^2 + m^2 + n^2 = 1 \tag{62}$$

and

$$l_1 l_2 + m_1 m_2 + n_1 n_2 = \cos\theta \tag{63}$$

where θ is the angle between the direction of incidence and the direction of scattering. Thus only the direction cosines with respect to the z-axis

$$n_1 = \cos\gamma_1 \qquad \text{and} \qquad n_2 = \cos\gamma_2 \tag{64}$$

remain explicitly. The z-axis is assumed parallel to the direction of the magnetic field lines. The longitudinal dimension

of the irregularities in the direction of the field lines is characterized by the scale length or correlation length L. The irregularities are assumed circularly symmetric about the z-axis with a transverse scale length T in the xy-plane.

Substitution of (64) in equation (60a) and using

$$(65) \qquad n = n_2 - n_1 = \cos \gamma_2 - \cos \gamma_1$$

$$= 2 \sin \tfrac{1}{2}(\gamma_2 + \gamma_1) \sin \tfrac{1}{2}(\gamma_2 - \gamma_1)$$

$$= 2 \sin \gamma \sin \tfrac{1}{2} \theta$$

where $\gamma_2 + \gamma_1 = 2\gamma$, $\gamma_2 - \gamma_1 = \theta$

gives

$$(66) \qquad P(\theta,\gamma) = (2\pi)^{3/2} T^2 L \; e^{-2k^2(T^2\cos^2\gamma + L^2\sin^2\gamma)\sin^2\theta/2}$$

From the last equation we have for:

Transverse Forward Scatter

$$(67a) \qquad n = n_2 - n_1 = 0$$

$$(67b) \qquad P(\theta_T,0) = (2\pi)^{3/2} T^2 L \; e^{-2k^2T^2\sin^2\theta_T/2}$$

independent of the angle of incidence, γ_1, and for:

Longitudinal Forward Scatter

$$(68a) \qquad n = 2 \sin \gamma \sin \tfrac{1}{2}\theta_L$$

$$(68b) \qquad P(\theta_L,\gamma) = (2\pi)^{3/2} T^2 L \; e^{-2k^2(T^2\cos^2\gamma + L^2\sin^2\gamma)\sin^2\theta_L/2}$$

The autocorrelation function describing the electron density deviations in the field-aligned irregularities is

$$(69) \qquad R(x,y,z) = e^{-\frac{1}{2}\left[(x^2+y^2)/T^2 + z^2/L^2\right]}$$

The electron density contour corresponding to: $R(x,y,z) = e^{-1}$, in a plane with normal: (l, m, n), is an ellipse since any diametral plane cuts the oblate spheroid

$$(70) \qquad (x^2+y^2)/T^2 + z^2/L^2 = 2$$

in an ellipse. The plane z = 0, normal to the direction of incidence (0, 0, 1), intersects (70) in the circle

$$(71a) \qquad x^2/T^2 + y^2/T^2 = 2$$

while the plane, y = 0, intersects (70) in the ellipse

$$(71b) \qquad x^2/T^2 + z^2/L^2 = 2$$

and in general the plane: $lx + my + nz = 0$ intersects (70) in an ellipse whose projection on the xy-plane, say, is the ellipse

$$(71c) \qquad Ax^2 + 2Bxy + Cy^2 - 2n^2 = 0$$

with

$$A = (n/T)^2 + (l/L)^2, \quad B = lm/L^2, \quad C = (n/T)^2 + (m/L)^2.$$

If an arbitrary semi-diameter of the intersection between (70) and the plane: $lx + my + nz = 0$, is denoted by r and has the direction cosines: (l', m', n'), then

$$(72) \qquad 1/r^2 = (l'^2+m'^2)/T^2 + n'^2/L^2$$

with $\qquad ll' + mm' + nn' = 0$

The electron density contour acting as aperture for the scatter beam is an ellipse with semi-axes r_1, r_2 and area:

$$(73) \qquad \pi r_1 r_2 = 2\pi T^2 L / \sqrt{(T^2 l^2 + T^2 m^2 + L^2 n^2)} \quad .$$

The angular power distribution in the resulting cone of scattered radiation is given by the formula (60a) for $P(\theta,n)$ or the equivalent formula for $P(k\, l_2-l_1,\ m_2-m_1,\ n_2-n_1)$. The equipower contour corresponding to: $P(\theta,n)$ = constant x e^{-1}, may be represented by the intersection of the scatter cone and the plane: $l_1 x + m_1 y + n_1 z = 1$, say. This contour is a plane curve which according to equations (67b) and (68b) for small angles, θ, is defined by

$$(74a) \qquad k^2 T^2 \theta_T^2 + k^2 (T^2 \cos^2\gamma + L^2 \sin^2\gamma)\theta_L^2 = 2$$

The last equation represents an ellipse with semi-axes

$$(74b) \qquad \theta_1 = \sqrt{2}/kT$$

$$(74c) \qquad \theta_2 = \sqrt{2}/k\sqrt{(T^2 \cos^2\gamma + L^2 \sin^2\gamma)}$$

Let $L = \rho T$

Then the axis ratio θ_1/θ_2 is given by

$$(75a) \qquad \theta_1/\theta_2 = \sqrt{(\cos^2\gamma + \rho^2 \sin^2\gamma)}$$

and we find that for

$$(75b) \qquad \gamma = 0 \quad : \qquad \theta_1/\theta_2 = 1$$

$$(75c) \qquad \gamma = \pi/4 \quad : \qquad \theta_1/\theta_2 = \sqrt{(1+\rho^2)}/\sqrt{2}$$

$$(75d) \qquad \gamma = \pi/2 \quad : \qquad \theta_1/\theta_2 = \rho$$

These results confirm the statements made in subsection 4.

6. Multiple Forward Scattering By Anisotropic Irregularities

6.1 Approach

The problem we need to consider is the transmission of radiation through a thick, plane-parallel layer containing anisotropic dielectric irregularities acting as scatterers of the incident radiation field. We are interested in the emerging radiation field at the bottom of the layer which in general will consist of the directly transmitted, attenuated radiation (undeviated component) and the scatter radiation (deviated components). Since the directly transmitted component is of importance to us as well as the scattered radiation, we are actually concerned with a problem of multiple diffraction rather than multiple scattering.

The problem we have described is a time-honored one in astrophysics where it is treated under the name of the theory of radiative transfer. The particular problem we are concerned with is radiative transfer in a purely scattering, plane-parallel, finite atmosphere with a constant net flux. The most complete treatment of the general theory is given by Chandrasekhar[26] in his book "Radiative Transfer". Van de Hulst[27] has discussed and classified into three types the available methods for solving multiple scattering problems. Specification of the state of polarization is accomplished by introduction of the Stokes' parameters for the intensity of the radiation field. This casts the equation of transfer into vector form.

It appears that the problem of scattering by anisotropic irregularities probably does not admit a solution in closed form,

but it can be solved in any finite approximation (Chandrasekhar, loc. cit., ch. X). The difficulty in the case of anisotropic scatterers is that the socalled phase matrix of the vector transfer equation or the phase function of the scalar transfer equation, corresponding to our function $P(\theta,n)$, is too complicated for a closed solution. Under these circumstances we have to decide to which order of approximation we desire a solution. Our present aim is to obtain an anlytical expression which in addition to describing the physical conditions with sufficient accuracy also is simple enough to be readily applicable to observations. If we limit ourselves to forward scatter by large, weak irregularities, we can use a simple method of approximation due to Fejer[7] which satisfies both requirements.

Fejer treated the case of small-angle multiple scattering in weak, isotropic irregularities. The thick, multiple scattering layer is divided into a number of thin, plane-parallel, singly scattering layers and an equation of transfer written for each. The phase function or angular power spectrum for single volume scattering can then be applied successively. The extension of this method to multiple scattering in a medium with anisotropic irregularities is simple because the radiative transfer equations are the same in both cases and only the phase function, $P(\theta)$, needs to be changed from Fejer's form (30') to the form (31') or (60a) appropriate for anisotropic scatterers.

We shall need a further extension of the theory to the case of two, separated, multiple scattering layers having anisotropic irregularities of different scale sizes. For the gaussian type

phase function we are concerned with this extension is straightforward although it does complicate the final expression for the emerging radiation somewhat.

6.2 Radiative transfer equation for forward scattering

The equation of radiative transfer will be stated in the usual astrophysical notation (cf. Chandrasekhar[26]). The equation of transfer for a plane-parallel atmosphere reads:

$$(76) \qquad (\cos \chi)\, dI_\nu(z,\chi,\phi)/\kappa_\nu dz = - I_\nu(z,\chi,\phi) + J_\nu(z,\chi,\phi)$$

where

I_ν = the specific intensity or spectral power density

κ_ν = the volume absorption (scattering) coefficient

J_ν = the source function = j_ν/κ_ν

j_ν = the volume emission coefficient

z = linear distance normal to the plane of stratification

χ = inclination to outward normal

ϕ = azimuth angle referred to the x-axis

ν = frequency, indicates radiation in the frequency interval $(\nu,\nu+d\nu)$.

The subscript, ν, will be omitted in the following for convenience.

For a purely scattering atmosphere the source function is of the form

$$(77) \qquad J(\underline{r},\underline{s}) = (1/4\pi) \int p(\underline{s},\underline{s}')\ I(\underline{r},\underline{s}')\, d\Omega_{s'},$$

where $\underline{s}$ is a unit vector denoting some direction through a point $\underline{r}$, $p(\underline{s},\underline{s}')$ a phase function normalized to unity, and Ω a solid angle.

We introduce the normal optical thickness, τ , measured inward from the boundary, and defined by

$$(78) \qquad d\tau = \kappa\, dz \quad , \quad \tau(z,z') = \int_{z'}^{z} \kappa\, dz$$

The equation of transfer may then be written as

$$(79) \qquad dI/d\tau \sec\chi = I - J$$

The formal solution of (79) is for the emerging intensities,

Outward:

(80a)

$$I(0,\chi,\phi) = I(\tau_1,\chi,\phi)e^{-\tau_1 \sec\chi} + \int_0^{\tau_1} J(t)e^{-t\sec\chi}\, dt \sec\chi$$

Inward:

(80b)

$$I(\tau_1,\chi,\phi) = I(0,\chi,\phi)e^{-\tau_1 \sec\chi} + \int_0^{\tau_1} J(t)e^{-(\tau_1 - t)\sec\chi}\, dt \sec\chi$$

The first term on the right hand side of (80b) is the attenuated, incident radiation and the integral gives the forward scattered radiation, as they emerge at the bottom of a layer of optical thickness τ_1. This formal solution becomes a solution to a physical problem when we specify a phase function and solve the resulting integral equation for I. One approach to the problem of solution is to replace the integral equation by an equivalent system of differential equations, and this is the method adopted by Fejer[7].

The analysis is based on the following suitable assumptions:

(1). A rectangular coordinate system O-xyz.

(2). A thick slab of material with random dielectric irregularities, delimited by the planes $z = z_0$ and $z = z_1$, and of thickness much larger than the scale length, ℓ.

(3). The mean capacitivity, $\overline{\epsilon}$, is the same inside and outside the slab.

(4). The rms deviation of the capacitivity, $(\Delta\epsilon)_{rms}$, is a function of z only.

(5). $\overline{(\Delta\epsilon)^2}$ varies sufficiently slowly so that there is no stratification within a single irregularity.

(6). A plane wave of intensity (power density) I_o is incident on the plane $z = z_0$ from the negative z-direction at an angle X with the z-axis.

It should be noted that the last condition will reverse the signs in the equation of transfer (79).

The equation of transfer for the first, singly scattering, elementary layer is

$$(81a) \qquad dI_1/d\tau \sec X = -I_1 + J_1$$

or

$$(81b) \qquad dI_1/ds = -I_1$$

with $ds = d\tau \sec X$ and $J_1 = 0$

and has the solution

$$(81c) \qquad I_1 = I_o e^{-s}$$

The equation of transfer for the second, elementary slab is

$$(82) \qquad dI_2/ds = -I_2 + J_2$$

$$= -I_2 - dI_1/ds$$

$$= -I_2 + I_1$$

and for the p-th slab we have similarly

$$(83) \qquad dI_p/ds = -I_p + I_{p-1}$$

This system of differential equations has the following solution for $z = z_1$ or $\tau = \tau_1$

$$(84) \qquad I_1 = I_o e^{-s_1}$$

$$I_2 = I_o s_1 e^{-s_1}$$

$$\cdots\cdots\cdots\cdots\cdots$$

$$I_p = I_o s_1^p e^{-s_1}/p!$$

$$\cdots\cdots\cdots\cdots\cdots$$

where $s_1 = \tau_1 \sec\chi$.

Addition of both sides gives

$$I_1 + I_2 + .. + I_p + .. = I_o e^{-s_1}(1 + s_1 + .. + s_1^p/p! + ..)$$

$$= I_o e^{-s_1} e^{s_1}$$

so the solution satifies the condition

$$(85) \qquad I_o = I_1 + I_2 + \cdots + I_p + \cdots$$

It will be seen that the approximation involved consists in putting the source function, J, equal to the scattered radiation emerging from each preceding, elementary slab

$$(86a) \qquad J_p = -dI_{p-1}/ds = I_{p-1}$$

which means that the backscattered radiation is ignored. For isotropic scatterers we have from (52) and (54b)

$$(86b) \qquad \sigma_B/\sigma_F = e^{-(k\ell)^2} \qquad \text{When} \quad k\ell \gg 1$$

Similarly, for anisotropic scatterers, with $L > T$,

$$(86c) \qquad \sigma_B/\sigma_F = e^{-2k^2(T^2\cos^2\gamma + L^2\sin^2\gamma)}$$

or

$$(86d) \qquad \sigma_B/\sigma_F \leq e^{-2(kT)^2} \qquad \text{When} \quad kT \gg 1$$

For $kT \geq 2$ we have $\sigma_B/\sigma_F < \frac{1}{2} \times 10^{-4}$

which shows that the approximation reflects the actual physical situation to a high degree of accuracy under the stated conditions.

The final expression for the emerging intensity at $z = z_1$ is of the form

$$(87) \qquad I = I_o e^{-s_1} + \sum_{p=1}^{\infty} I_p P_p(\theta)$$

and it remains to find the expression for the angular power spectrum after p-times scattering, $P_p(\theta)$.

6.3 Angular power spectrum after multiple scattering

Consider two plane-parallel, singly scattering layers which need not be adjacent and may contain anisotropic irregularities characterized by different scale lengths T_1, L_1 and T_2, L_2 in layer 1 and layer 2 respectively.

Let:

The direction cosines of a plane wave incident on layer 1 be

(88a) $$(l_o, m_o, n_o)$$

The angular power spectrum of the plane wave after scattering in layer 1 be

(88b) $$P_1(l_{10}, m_{10}, n_{10})$$

The angular power spectrum of the same plane wave incident on layer 2, after scattering in layer 2, be

(88c) $$P_2(l_{20}, m_{20}, n_{20})$$

The angular power spectrum of the plane wave after successive scattering in layers 1 and 2 be

(88d) $$P(l_{20}, m_{20}, n_{20})$$

The notation (l_{10}, m_{10}, n_{10}) stands for $(l_1-l_o, m_1-m_o, n_1-n_o)$, etc., and is to be understood in the sense of equations (24) and (31a').

Then the angular power spectrum of the plane wave after successive scattering in the layers 1 and 2 is the convolution of P_1 and P_2:

(89a) $$P = P_1 * P_2$$

with

(89b) $$P_1 = (2\pi)^{3/2} T_1^2 L_1 \, e^{-\frac{1}{2}k^2 T_1^2 (l^2+m^2)} \, e^{-\frac{1}{2}k^2 L_1^2 n^2}$$

(89c) $$P_2 = (2\pi)^{3/2} T_2^2 L_2 \, e^{-\frac{1}{2}k^2 T_2^2 (l^2+m^2)} \, e^{-\frac{1}{2}k^2 L_2^2 n^2}$$

The evaluation of the convolution integral is elementary, and the resulting expression for P reads

$$P = C\, e^{-\frac{1}{2}k^2T^2(l_{20}^2+m_{20}^2)}\; e^{-\frac{1}{2}k^2L^2n_{20}^2} \tag{90a}$$

or

$$P = C\, e^{-2k^2T^2\sin^2\theta/2}\; e^{-\frac{1}{2}k^2(L^2-T^2)\,(n_2-n_o)^2} \tag{90b}$$

where

$$C = (2\pi)^{3/2}/k^3(T_1^2+T_2^2)\sqrt{(L_1^2+L_2^2)} \tag{90c}$$

$$T^2 = T_1^2T_2^2/(T_1^2+T_2^2) \quad , \quad L^2 = L_1^2L_2^2/(L_1^2+L_2^2) \tag{90d}$$

Comparison of (90b) with (31b') shows that the angular power spectrum has the same <u>form</u> after a single and two scatterings as might be expected.

If we now put: $T_1 = T_2 = T$ and $L_1 = L_2 = L$,

we see that after two scatterings in adjacent, elementary slabs of a single layer the angular power spectrum is

$$P_{(2)} = C_2\, e^{-2(k^2/2)T^2\sin^2\theta/2}\; e^{-\frac{1}{2}(k^2/2)(L^2-T^2)n_{20}^2} \tag{91}$$

and similarly, after p scatterings we have

$$P_{(p)} = C_p\, e^{-2(k^2/p)T^2\sin^2\theta/2}\; e^{-\frac{1}{2}(k^2/p)(L^2-T^2)n_{20}^2} \tag{91a}$$

where

$$C_p = (\pi/k^2)^{3p/2}\, T^2L$$

The above expressions for the angular power spectrum of the p-times scattered wave in a thick layer with weak, anisotropic irregularities reduces to Fejer's equation (38) for the angular power spectrum after multiple scattering in weak, isotropic irregularities if we let

$$\bar{T} = \bar{L} = \ell/\sqrt{2} \qquad \text{and} \qquad \sin^2\theta/2 = \theta^2/4$$

Examination of the expressions (89d) for $\bar{T}^2$ and $\bar{L}^2$

$$\bar{T}^2 = \bar{T}_1^2\bar{T}_2^2/(\bar{T}_1^2+\bar{T}_2^2) \quad , \quad \bar{L}^2 = \bar{L}_1^2\bar{L}_2^2/(\bar{L}_1^2+\bar{L}_2^2)$$

show that $\bar{T}^2$ and $\bar{L}^2$ are (half) the harmonic means of respectively $\bar{T}_1^2$, $\bar{T}_2^2$ and $\bar{L}_1^2$, $\bar{L}_2^2$. It will therefore be convenient to introduce the reciprocal scale lengths or related parameters.

We have shown earlier that n_{20} may be written as

(92a) $$n_{20} = n_2 - n_o = 2 \sin\gamma \sin\theta_L/2$$

with $$\gamma = (\gamma_2 + \gamma_o)/2 \quad , \quad \theta_L = \gamma_2 - \gamma_o$$

We also have from spherical trigonometry that

(92b) $$\cos\theta = \cos\theta_T \cos\theta_L$$

or

(92c) $$\sin^2\theta/2 = \sin^2\theta_T/2 + \sin^2\theta_L/2 - 2\sin^2(\theta_T/2)\sin^2(\theta_L/2)$$

$$\doteq \sin^2\theta_T/2 + \sin^2\theta_L/2 - 4\sin^4\theta/2$$

Therefore P may be written as

$$(93) \qquad P = C\, e^{-2k^2\bar{T}^2\sin^2\theta/2}\; e^{-2k^2(L^2-\bar{T}^2)\sin^2\gamma\,\sin^2\theta_L/2}$$

$$= C\, e^{-2k^2\bar{T}^2\sin^2\theta_T/2}\; e^{-2k^2(\bar{T}^2\cos^2\gamma+L^2\sin^2\gamma)\sin^2\theta_L/2}$$

$$\times\; e^{-4k^2(L^2-\bar{T}^2)\sin^2\gamma\,\sin^4\theta/2}$$

or

$$(94a) \qquad P = C\, e^{-4(\sin^2\theta_T/2)/t^2}\; e^{-4(\sin^2\theta_L/2)/\ell^2}$$

with

$$(94b) \qquad t^2 = 2/k^2\bar{T}^2$$

$$(94c) \qquad \ell^2 = 2/k^2(\bar{T}^2\cos^2\gamma + L^2\sin^2\gamma)$$

and ignoring the term with $\sin^4\theta/2$ in the exponent.

For small forward scatter angles, θ, we have with $4\sin^2\theta/2 \doteq \theta^2$

$$(95a) \qquad P_j = C_j\, e^{-\theta_T^2/t_j^2}\; e^{-\theta_L^2/\ell_j^2} \quad , \quad j = 1,2$$

where

$$(95b) \qquad t_j^2 = 2/k^2\bar{T}_j^2$$

$$(95c) \qquad \ell_j^2 = 2/k^2(T_j^2\cos^2\gamma_j + L_j^2\sin^2\gamma_j) \;,\; \gamma_j = (\gamma_j+\gamma_o)/2$$

In terms of the parameters t_j, ℓ_j we have from (89b,c) and (90a) that when a plane wave is scattered by the elementary slab 1 into the angular spectrum

$$(96a) \qquad P_1 = C_1\, e^{-\theta_T^2/t_1^2}\; e^{-\theta_L^2/\ell_1^2}$$

and the same plane wave is scattered by the elementary slab 2 into the angular spectrum

$$P_2 = C_2 e^{-\theta_T^2/t_2^2} e^{-\theta_L^2/\ell_2^2} \tag{96b}$$

then successive scattering by the slabs 1 and 2 produces the angular power spectrum

$$P = C e^{-\theta_T^2/(t_1^2 + t_2^2)} e^{-\theta_L^2/(\ell_1^2 + \ell_2^2)} \tag{96c}$$

The angular power spectrum resulting from multiple scattering in two separate, thick layers with anisotropic irregularities having different scale lengths T_1, L_1 and T_2, L_2 is now easily deduced.

The angular power spectrum produced by the first scattering of the incident plane wave in the layer 1 is for small angles, θ:

$$P_{(1)} = C_1 e^{-\theta_T^2/t_1^2} e^{-\theta_L^2/\ell_1^2} \tag{97a}$$

and after p scatterings in layer 1 the angular spectrum is:

$$P_{(p)} = C_p e^{-\theta_T^2/pt_1^2} e^{-\theta_L^2/p\ell_1^2} \tag{97b}$$

If this angular power spectrum is incident on layer 2, then after one scattering in this layer we have the angular spectrum:

$$P_{(p,1)} = C_{p,1} e^{-\theta_T^2/(pt_1^2 + t_2^2)} e^{-\theta_L^2/(p\ell_1^2 + \ell_2^2)} \tag{97c}$$

and after q scatterings in layer 2 we have the angular power spectrum:

$$(97d) \qquad P_{(p,q)} = C_{p,q}\, e^{-\theta_T^2/(pt_1^2 + qt_2^2)}\, e^{-\theta_L^2/(p\ell_1^2 + q\ell_2^2)}$$

or

$$(98a) \qquad P_{(p,q)} = C_{p,q}\, e^{-\frac{k^2}{2}\theta_T^2\, T_1^2T_2^2/(pT_2^2 + qT_1^2)} \times e^{-\frac{k^2}{2}\theta_L^2\, K_1^2K_2^2/(pK_2^2 + qK_1^2)}$$

where

$$(98b) \qquad K_1^2 = T_1^2 \cos^2\gamma_1 + L_1^2 \sin^2\gamma_1$$

$$(98c) \qquad K_2^2 = T_2^2 \cos^2\gamma_2 + L_2^2 \sin^2\gamma_2$$

The quantities

$$T_1^2T_2^2/(pT_2^2 + qT_1^2) \quad , \quad K_1^2K_2^2/(pK_2^2 + qK_1^2)$$

are weighted harmonic means of respectively T_1^2, T_2^2 and K_1^2, K_2^2.

In applications of these formulas to interferometer observations of radio star visibility fades we shall usually be interested in the transverse scatter angle, θ_T, only, although occasionally in the longitudinal scatter angle, θ_L, but seldom in both θ_T and θ_L simultaneously.

The above results for the convolution of two or more angular power spectra will also be useful for ascertaining precisely the

consequences of replacing the incident plane wave radiation from a fictitious point source at infinite distance by either the radiation from an extended source at essentially infinite distance (radio star) or a point source at a finite distance (artificial satellite).

6.4 The solution for the multiple scattering problem

The solution of the radiative transfer equation for the intensity of the radiation transmitted through a thick, multiple scattering layer can now be found by combination of the equations (77), (87), (97b) and (92c). We have from (77), with $\cos X = \mu$,

(99a)

$$J_{p+1} = (1/4\pi) \int_{-1}^{+1} \int_{0}^{2\pi} P_p(\mu,\phi,\mu',\phi')\, I_p(s,\mu,\phi,\mu',\phi')\, d\mu' d\phi'$$

$$= I_p(s,\mu_o,\phi_o)$$

by the mean value theorem. In order that the normalized phase function, $P_p(\theta)$, be independent of the azimuth angle, ϕ, the coordinate system O-xyz must have its z-axis parallel to the direction of the magnetic field lines. Therefore X is identical with the angle γ introduced earlier. This implies that the ionosphere is assumed to be stratified in plane-parallel layers normal to the magnetic field lines rather than normal to the vertical through astronomical zenith. For auroral zone latitudes the difference is slight since the angular distance of magnetic zenith from astronomical zenith is in the range 11-14°.

For the purpose of evaluating the integral (99a) it is convenient to write $P_p(\theta)$ on the form

(99b) $$P_p(\theta) = C_p\, e^{-(2/p\ell_1^2)(1-\cos\theta)}\, e^{(2/pa_1^2)\sin^2\theta_T/2}$$

with

(99c) $$1/a_1^2 = k^2(L_1^2-T_1^2)\sin^2\gamma_1$$

Then the normalization condition

(99d) $$(1/4\pi)\int_0^{2\pi}\int_{-1}^{1} C_p\, e^{-(2/p\ell_1^2)(1-\mu)}\, e^{(2/pa_1^2)\sin^2\theta_T/2}\, d\mu\, d\phi = 1$$

gives

(99e) $$C_p = (4/p\ell_1^2)\, e^{-(2/pa_1^2)\sin^2\theta_T/2}$$

$$= (2k^2/p)(T_1^2\cos^2\gamma_1 + L^2\sin^2\gamma_1)\, f_p(\sin\theta_T)$$

ignoring the term $e^{-4/p\ell_1^2}$. If we use the small angle approximation

(99f) $$P_p = C_p\, e^{-\theta^2/p\ell_1^2}\, e^{\theta_T^2/pa_1^2}$$

and

(99g) $$(1/4\pi)\int_0^{2\pi}\int_0^{\infty} C_p\, e^{-\theta^2/p\ell_1^2}\, e^{\theta_T^2/pa_1^2}\,\theta\, d\theta\, d\phi = 1$$

we find

(99h) $$C_p = (1/p\ell_1^2)\, e^{-\theta_T^2/pa_1^2}$$

which for: $T = L = \ell/\sqrt{2}$ reduces to Fejer's corresponding equation for isotropic irregularities:

$$(99i) \qquad C_p = \pi^2 \ell^2 / \lambda^2 p$$

The solution for the emerging intensity after multiple scattering in layer 1 is

$$(100) \qquad I(s_1, X, \phi) = \bar{I}_o e^{-s_1} + \sum_{p=1}^{m} \bar{I}_o e^{-s_1} (s_1^p/p!) P_p(\theta)$$

with $\bar{I}_o = \bar{I}(0, X, \phi)$ and $s_1 = \tau_1 \sec X$, where

$$(100a) \qquad P_p(\theta) = (4/p\ell_1^2) e^{-(2/p\ell_1^2)\sin^2\theta/2} f_p(\sin\theta_T)$$

or

$$(100b) \qquad P_p(\theta) = (1/p\ell_1^2) e^{-\theta^2/p\ell_1^2} f_p(\theta_T)$$

or

$$(100c) \qquad P_p(\theta) = (1/p\ell_1^2) e^{-\theta_T^2/pt_1^2} e^{-\theta_L^2/p\ell_1^2} f_p(\theta_T, \theta_L)$$

and with

$$(100d) \qquad f_p(\sin\theta_T) = e^{-(2k^2/p)(L_1^2 - T_1^2)\sin^2\gamma_1 \sin^2\theta_T/2}$$

$$(100e) \qquad f_p(\theta_T, \theta_L) = e^{-(\theta_T^2 k^2/2p)(L_1^2 - 2T_1^2)\sin^2\gamma_1}$$

The factors f_p equal unity for $\gamma_1 = 0$ and will often be sufficiently close to unity to be ignored. The solution reduces to Fejer's solution for multiple scattering of a plane wave normally incident on a thick layer with isotropic irregularities if we let $T = L = \ell/\sqrt{2}$ and $\chi = 0$.

The intensity of the radiation emerging after multiple scattering in a second, thick, plane-parallel layer is readily deduced by repetition of the procedure for layer 1, using the expression (100) for the intensity of the incident radiation. Denote the diffracted radiation, $I(s_1,\chi,\phi)$, emerging from layer 1 by I'. Then we have for the first elementary slab of layer 2 the equation of transfer

$$dI'_1/ds = -I'_1 \tag{101a}$$

and for the q-th elementary slab

$$dI'/ds = -I'_q + I'_{q-1} \tag{101b}$$

where, $ds = d\tau \sec \chi$, as before. The solutions for $z' = z'_2$ or $\tau = \tau_2$, in a coordinate system O'-$x'y'z'$ shifted along the z-axis ($x'=x$, $y'=y$, $z'=z-c$, $c \geq z_1$), are

$$I'_1 = I'_o e^{-s_2} \tag{102}$$

$$\cdots\cdots\cdots\cdots\cdots$$

$$I'_q = I'_o e^{-s_2} s_2^q/q!$$

$$\cdots\cdots\cdots\cdots\cdots\cdots\cdots$$

so the solution for the emerging intensity, I'', is

$$(103a) \qquad I'' = I_o' e^{-s_2} + \sum_{q=1}^{n} I_q' P_q'(\theta)$$

with

$$(103b) \qquad P_q'(\theta) = C_q' e^{-\theta^2/q\ell_2^2} f_q'(\theta_T)$$

The normalized phase function for a wave scattered p times in layer 1 and q times in layer 2 is

$$(104a) \qquad P_{pq}(\theta) = (p\ell_1^2+q\ell_2^2)^{-1} e^{-\theta^2/(p\ell_1^2+q\ell_2^2)} f_{pq}(\theta_T)$$

with

$$(104b) \qquad f_{pq}(\theta_T) = e^{-\theta_T^2/(pa_1^2+qa_2^2)}$$

$$(104c) \qquad 1/a_j^2 = (k^2/2)(L_j^2-T_j^2)\sin^2\gamma_j \quad , \quad j = 1,2$$

The complete solution for the emerging intensity after multiple scattering in two layers reads

(105)

$$I(s_2,\chi,\phi) = I_o e^{-(s_1+s_2)} + \sum_{q=1}^{n}\sum_{p=0}^{m} I_o e^{-(s_1+s_2)} (s_1^p s_2^q/p!q!) P_{pq}(\theta)$$

with $I_o = I(0,\chi,\phi)$, $s_1 = \tau_1 \sec \chi$, $s_2 = \tau_2 \sec \chi$.

For large magnetic zenith angles, χ greater than 50°, say, a correction for layer curvature must be made. The corrected secant factor, $\sec \chi'$, is given by

$$(106) \qquad \sec \chi' = (1 + h/r_o)/\sqrt{(\cos^2\chi + 2h/r_o + h^2/r_o^2)}$$

where h is the height of the ionospheric layer above ground and r_o is the radius of the earth.

When the number of scatterings in one or both of the layers is large, useful approximate expressions for (100) or (105) can be found. Application of Stirling's formula to (84):

$$I_p = I_o e^{-s_1} (s_1^p/p!)$$

gives

$$(107) \qquad I_p \doteq I_o (2\pi p)^{-1/2} e^{p-s_1} (s_1/p)^p$$

Logarithmic differentiation of this expression shows that it has a maximum when

$$p\, e^{-2p} = s_1 \qquad \text{or} \qquad p \doteq s_1 \qquad \text{for} \qquad p \gg 1 .$$

Similarly,

$$I'_q = I_o e^{-s_2} (s_2^q/q!) = I_o e^{-(s_1+s_2)} (s_1^p s_2^q/p!q!)$$

has a maximum when

$$p \doteq s_1 \qquad \text{and} \qquad q \doteq s_2 \qquad \text{for} \qquad p \gg 1 \ , \ q \gg 1 .$$

The maximum is sharp for large p, or large p and q. Therefore, when the number of scatterings is large, the main features of the emerging field, and in particular the angular distribution of intensity, may be estimated from the following approximate expressions

$$(108) \qquad I' \doteq I_o e^{-s_1} + I_o e^{-s_1} (s_1^p/p!)\, P_p(\theta)$$

with $\quad p \doteq s_1 >> 1$

$$(109) \qquad I'' \doteq I_o e^{-(s_1+s_2)} + I_o e^{-(s_1+s_2)} (s_1^p s_2^q/p!q!)\, P_{pq}(\theta)$$

with $\quad p \doteq s_1 >> 1 \qquad$ and $\qquad q \doteq s_2 >> 1$

These expressions can be simplified further by use of Stirling's formula.

7. Diffracting Screen. Fresnel and Fraunhofer Diffraction

The diffraction effects of the ionosphere on radio transmissions from radio stars and satellites are frequently represented in terms of a thin, plane, phase-changing diffracting screen. The diffraction field resulting from multiple scattering in a thick layer may be simulated by the effect of an equivalent screen of this type. For such representations we need two-dimensional versions of the autocorrelation function of the kind resulting from intersecting the three-dimensional function (70) for the electron density deviations with a plane, $lx + my + nz = 0$,

normal to a specified direction of incidence (l,m,n). In the special case of incidence parallel to the direction of the magnetic field lines, (l,m,n) = (0,0,1), we can write

$$(110) \qquad R(r) = e^{-(r/\ell)^2}$$

with $r^2 = x^2 + y^2$, and $\ell/\sqrt{2} = T$. Then Fejer's[7] discussion applies.

The point of interest is that the autocorrelation function, R, may be represented as a sum of the autocorrelation functions for the elementary scatterings

$$(111a) \qquad R = \sum_{p=0}^{m} R_p$$

with

$$(111b) \qquad R_p = (s_1^p/p!)\, e^{-s_1}\, e^{-pr^2/\ell^2}, \quad s_1 = \tau_1 \sec 0 = \tau_1$$

and the following approximations obtain.

For

$r \ll \ell$, dominant term: $p = \tau_1$, $R \doteq e^{-r^2\tau_1/\ell^2}$

$r \doteq \ell$, dominant term: $p = \tau_1/\ell$, $R \propto e^{-r^2\tau_1/e\ell^2}$

$r \to \infty$, dominant term: $p = 0$, $R = e^{-\tau_1}$

A comparison of this with the results by Hewish[28] for a thin, phase-changing screen shows that when

$$r \ll \ell \qquad \Delta\phi(r) = (r/\ell)\sqrt{(2\tau_1)}$$

$$r \doteq \ell \qquad \Delta\phi(\ell) = \sqrt{(2\tau_1/e)}$$

$$r \to \infty \qquad \Delta\phi(\infty) = \sqrt{(2\tau_1)}$$

where $\Delta\phi$ denotes the root-mean-square phase difference between two points in the equivalent phase-changing screen separated by the distance r. Now the diffraction effects caused by the plane, phase-changing screen depend only on ℓ if $\Delta\phi$ is less than one radian, but depend on $\ell/\Delta\phi$ if the rms phase deviations are larger than one radian. The upshot of this for a thick layer (and $r \doteq \ell$ or $r \to \infty$) is therefore that for τ_1 less than one, the diffraction effect depends only on the size, ℓ, of the irregularities, but it depends on $\ell/\sqrt{\tau_1}$ when τ_1 is larger than one. Thus multiple scattering in a thick layer with optical thickness less than unity is equivalent to diffraction in a phase-changing screen with rms phase deviations less than one radian. A multiple scattering layer with optical thickness larger than unity has as its equivalent a diffracting screen with rms phase deviations larger than one radian. The representation in terms of an equivalent, plane, phase-changing screen can clearly be extended to other angles of incidence, with proper allowance for curvature at large zenith angles. But we prefer the more direct approach based on the actual physical scattering process and shall not pursue the method of representation in terms of equivalent diffracting screens. The latter method has recently been discussed by Wagner[29] who extends the theory by Hewish for the case of a

shallowly phase-modulating screen to the case of a deeply phase-modulating screen.

An important consideration in the interpretation of the observed diffraction field is the distance between the diffracting layer or equivalent diffracting screen and the plane of observation. The distinction between the Fresnel and Fraunhofer diffraction regions which is made in this connection according as the wave field is observed near or far from the screen will be well known. Physically the situation is as follows. Close to a diffracting aperture the radiation is propagated rectilinearly in a column of the same cross-section and shape as the aperture. By and by amplitude or intensity fluctuations start to appear near the boundaries of this column. When the diffracted field is observed on a plane or second screen, these fluctuations give rise to fringes around the boundaries known as Fresnel fringes. With increasing distance from the diffracting screen, the size of the Fresnel fringes increases as the square root of the distance and in the end become so large that only one or two fringes remain in the pattern of the aperture. Finally the transition to the Fraunhofer diffraction region occurs, and the radiation column spreads out in a cone. The Fraunhofer pattern increases in size proportionally to the distance from the diffracting screen, and may be described in terms of the angular separation of the fringes. The distance at which the transition from Fresnel to Fraunhofer diffraction occurs is known as the Fresnel distance, z_F, and given by

$$z_F = d^2/\lambda \tag{112}$$

where d denotes the linear dimension of the aperture or diffracting obstacle.

For a scattering irregularity described by the autocorrelation function, $R(x,y,z) = \exp -\frac{1}{2}\left[(x^2+y^2)/T^2 + z^2/L^2\right]$, the Fresnel distance for the transverse scale length, T, is according to (57c)

$$z_F = 13\, T^2/\lambda \tag{113}$$

Assuming that a typical F layer irregularity has a transverse dimension of d = 600 meters and a typical E layer irregularity a transverse dimension of d = 150 meters, the corresponding Fresnel distances are

F layer: $z_F = 360 \times 10^3/\lambda$ meters

E layer: $z_F = 22.5 \times 10^3/\lambda$ meters

Conversely, the limits placed on the transverse size, d, and scale length, T, of the irregularities in order that the Fraunhofer pattern may have started to develop at distances of respectively 400 and 100 km from the F and E layers are

F layer: $d < 630\sqrt{\lambda}$ meters, $T < 175\sqrt{\lambda}$ meters

E layer: $d < 310\sqrt{\lambda}$ meters, $T < 88\sqrt{\lambda}$ meters .

These estimates are important for the interpretation of the diffracted radio star radiations observed on the ground. It should be noted that the distinction between Fresnel and Fraunhofer regions has a bearing only on the extent to which amplitude or intensity fluctuations have developed as the diffracted radiation

reaches the ground, and whether the radio star scintillations will appear mainly as amplitude or phase variations, or a mixture of both (see Ratcliffe[3]). The angular power spectrum of the diffracted field is completely developed as the radiation emerges from the diffracting layer or screen, and does not change with the distance from the screen.

8. Natural Sources of Radiation

The theory of single and multiple scattering of radio waves developed earlier assumes that the incident radiation may be represented as monochromatic, linearly polarized, plane waves such as would result from an ideal Hertzian dipole radiator located at an essentially infinite distance. Natural radiation does not possess these idealized properties, and in applications of the theory attention must therefore be given to possible effects of deviations from the ideal conditions. A general, comprehensive discussion of the interference and diffraction of real wave fields produced by finite, polychromatic sources has recently been given by Born and Wolf[30], so we need only consider a few specific points here.

The bright radio stars used for the experimental study of the auroral ionosphere reported in Section II are extended sources with angular diameters of a few minutes of arc, radiating unpolarized, random noise over the entire radio frequency spectrum. The linear polarization and narrow r-f characteristics of the receiving equipment ensure that the accepted radiation field has the polarization and quasi-monochromatic properties required by the theory. This may be seen as follows.

The state of polarization of any electromagnetic radiation is completely characterized by the four Stokes' parameters (see Chandrasekhar[26] or Born and Wolf[30]). Natural radiation may be decomposed into two independent oppositely polarized beams of equal intensity. The total intensity of a mixture of two oppositely polarized beams is not affected by relative phase retardations between the beams. This has the important consequence that the radiation in the two beams can never interfere with one another.

The degree of quasi-monochromacy of the received radiation is characterized by the ratio, $\Delta f/f_o$, of receiver bandwidth to center frequency. In the cases we are concerned with, this ratio is of the order of $10^{-2} - 10^{-3}$.

Our primary concern is therefore the effect of the finite size of the radio stars and other physical sources of radiation. Since no physical source can be a true point source, it is reasonable to introduce the concept of a quasi point source, and seek a measure of the degree to which the actual source may be said to represent a quasi point source. The proper measure of this is the degree of (partial) coherence existing between the radiations from different points of the finite source (see Born and Wolf[30]).

Let x denote the distance between two points, Q_1 and Q_2, located on a plane of observation, Q. If x is small compared with the distance of the source, or the distance to the image of the source on a diffracting screen, then the diameter of the circular area that is illuminated almost coherently by a

quasi-monochromatic uniform source of angular radius, α, is

(114a) $\quad x = 0.16\bar{\lambda}/\alpha \quad , \quad \bar{\lambda}$ = mean wavelength.

For a uniformly illuminated rectangular strip of angular half-width w the corresponding distance is

(114b) $\quad x = 0.13\bar{\lambda}/w$

The degree of coherence between the wave fields observed at Q_1 and Q_2 decreases steadily as the separation x increases, and complete incoherence is attained for

(115a) $\quad x' = 0.61\ \bar{\lambda}/\alpha'$ circular disk

(115b) $\quad x' = 0.5\ \bar{\lambda}/w'$ rectangular strip

For a given, fixed separation, x_o, the largest disk or strip which is almost coherently illuminated has the angular diameter or width

(116a) $\quad 2\alpha = 0.32\ \bar{\lambda}/x_o$ circular disk

(116b) $\quad 2w = 0.26\ \bar{\lambda}/x_o$ rectangular strip

There is complete incoherence if the disk or strip has the angular diameter or width

(117a) $\quad 2\alpha' = 1.22\ \bar{\lambda}/x_o'$ circular disk

(117b) $\quad 2w' = \quad \bar{\lambda}/x_o'$ rectangular strip

Intuitively we expect the extended source to represent a quasi point source when the angular diameter or width is less than, or equal to, that given by (116a,b), and that the effects of finite size will become increasingly important for objects of increasing angular dimensions exceeding the limits set by (116a,b). This qualitative statement can be made precise by evaluating

the angular power spectrum of the extended source in question, and deducing the differential effects resulting from use of the actual angular power spectrum and the delta-function angular power spectrum of a point source.

The normalized angular power spectrum of a circular disk with radius R, or rectangular strip of half-width W, having a uniform brightness (intensity) is respectively

(118a) $P(\sin\theta) = 2J_1(kR \sin\theta)/kR \sin\theta$, circular disk

(118b) $P(\theta) = 2J_1(kR\theta)/kR\theta$, for small angles θ

and

(119a) $P(\sin\theta) = \sin(kW \sin\theta)/kW \sin\theta$, rectangular strip

(119b) $P(\theta) = \sin(kW\theta)/kW\theta$, for small angles θ

Power series expansion of these expressions in terms of θ show that for small values of the argument there are convenient representations in terms of gaussian functions:

(120a)

$$P(\theta) = 1 - (\theta/2\theta_o)^2/2 + (\theta/2\theta_o)^4/2.3! - \ldots \doteq e^{-\theta^2/8\theta_o^2}$$

with $\theta_o = 1/kR$, and

(120b)

$$P(\theta) = 1 - (\theta/\theta_o)^2/3! + (\theta/\theta_o)^4/5! - \ldots \doteq e^{-\theta^2/6\theta_o^2}$$

with $\theta_o = 1/kW$.

In order to determine the value of the constant θ_o for a given source and observing (interferometer) system, let

$$\sin\theta = x/r \doteq \theta$$

with: r = distance to the source, x = separation of antennas or mirrors. The angular radius, α, or angular half-width, w, of the source is: $\alpha = R/r$, $w = W/r$.

Now

(121a)

$$P(x) = 2J_1(k\alpha x)/k\alpha x = 2J_1(\alpha/\alpha_o)/(\alpha/\alpha_o) \doteq e^{-\alpha^2/8\alpha_o^2}$$

(121b)

$$P(x) = \sin(kwx)/kwx = \sin(w/w_o)/(w/w_o) \doteq e^{-w^2/6w_o^2}$$

with $\alpha_o = w_o = 1/kx = \lambda/2\pi x = 1/2\pi x_\lambda$.

The equivalent strip, angular widths of the radio stars Cassiopeia A and Cygnus A are respectively (Shakeshaft et al.[31])

Cas A:	3.'8	or	0.0011	radians
Cyg A:	2.'3	or	0.0007	radians

The value of θ_o corresponding to the angular half-width 1.'9 is:

$$\theta_o = 0.0009$$

The maximum antenna separation for almost coherent illumination over a strip of (half) width 1.'9 , measured in wavelengths, is

$$x_\lambda = 177$$

We can now use the results of subsection 6 to estimate the number of multiple scatterings which the radiation from a point

source must undergo in order to spread out in an angular spectrum matching that of a radio star. This is not by itself sufficient to make the two radiation beams equivalent, but if the directly transmitted component of the point source radiation is simultaneously attenuated sufficiently in the multiple scattering layer, then equivalence is attained.

We have from equations (100b) with (95c) and (120b)

$$6\theta_o^2 = p\ell_1^2 = 2p/(kT)^2 \tag{122a}$$

$$p = 3(\theta_o kT)^2 = 9(\theta_o \times 3.6T)^2/\lambda^2 \tag{122b}$$

For Cas A, which has the larger disk of the two brightest radio stars, we find that

$$p = 7.29 \times 10^{-6} (3.6\ T)^2/\lambda^2 \tag{123}$$

For a transverse irregularity dimension of 600 meters this gives (scale length $T = 600/3.6$)

$$p = 2.6/\lambda^2 \tag{124}$$

or one scattering for wavelengths equal to, or larger than, 1.6 meters (frequencies $\leq$ 185 Mc/s). If the transverse irregularity length is 200 meters, we find

$$p = 0.3/\lambda^2 \tag{125}$$

or one scattering for $\lambda \geq 0.55$ meters ($f \leq 550$ Mc/s).

The effect of the finite size of the radio source Cas A can now be ascertained. Assume that the radiation from an infinitely distant point source traverses a multiple scattering layer of optical thickness equal to or greater than one, which has

irregularities with transverse dimensions of 400 meters or less, and that the radiation is scattered ten times or more. Then, at any very-high frequency, the effect of replacing the incident radiation from the point source with that from the finite source Cas A, is to reduce by no more than one the number of scatterings required to produce the same emerging diffracted field. Therefore, the error in the estimated number of scatterings, and hence the thickness of the multiple scattering layer, resulting from ignoring the finite size of the source, will be ten per cent or less.

This indicates that in most practical cases a finite source of angular size less than the almost coherently illuminated disk may be considered to be a quasi point source, and the finite extent ignored. If desired, and in the exceptional cases, the effect of the finite source can be ascertained and removed by evaluation of its angular power spectrum and use of the convolution law. This law states that if the angular power spectrum of the diffracted point source field is

$$P_d(\theta) \propto e^{-\theta^2/\theta_d^2} \tag{126a}$$

and the angular power spectrum of the finite source is

$$P_s(\theta) \propto e^{-\theta^2/\theta_s^2} \tag{126b}$$

then the resultant, observed angular power spectrum will be

$$P(\theta) \propto e^{-\theta^2/(\theta_d^2 + \theta_s^2)} . \tag{126c}$$

When the angular power spectrum of the source is known, or can be estimated, a correction for the finite size of the source can easily be applied to the observations.

For a radio star visibility fade observed with an interferometer, the angular power spectrum is determined by the condition (see subsection 10)

$$\theta^2/(\theta_d^2 + \theta_s^2) = 1 \tag{127a}$$

or

$$\theta_d^2 = \theta^2 - \theta_s^2 = \theta^2(1 - \theta_s^2/\theta^2) \tag{127b}$$

where

$$\theta_d^2 = 2p/(kT)^2 \quad , \quad \theta_s^2 = 6\theta_o^2 \tag{127c}$$

so

$$p = \tfrac{1}{2}(kT\theta)^2(1 - \theta_s^2/\theta^2) \tag{128}$$

Here θ has a magnitude corresponding to the angular width of the strip giving complete incoherence, $2w'$, while θ_s has a magnitude of the order of the almost coherently illuminated strip, $2w$. Since $w/w' \doteq 1/4$, the correction factor $(1 - \theta_s^2/\theta^2)$, taking account of the finite size of the source, is of the order of 0.9 - 0.95. This indicates a 5-10 per cent correction to the value for p obtained by regarding the radio star as a point source, provided that the optical thickness of the scattering layer and p is sufficiently large.

9. Limitations of the Theory

A correct application of the foregoing theory for radio wave scattering to actual situations requires an appreciation of the

conditions under which it may be expected to work and its inherent limitations. We note first that it is a weak scattering theory based on a Born approximation. This means that the observing frequency must always be considerably larger than the highest plasma frequency encountered in the medium. For auroral ionization the plasma frequency is in the range 3-30 Mc/s, with 10 Mc/s as a typical peak value under average auroral activity. Therefore the theory will generally be applicable to VHF and UHF, but not HF radiations. During strong auroral activity use of the theory for exploring radio waves below 50-60 Mc/s, say, is questionable. The Born approximation approach poses no problems beyond such frequency limitations, that is, a weak scattering theory is considered to give an adequate and proper description of the interaction of VHF-UHF radio waves with the auroral ionization.

The mathematical development and discussion of the theory of single scattering in weak irregularities in subsections 2 and 3 shows that the assumptions imposing the most serious limitations for applications are:

Ass. 4 The relative deviations $\Delta\epsilon/\epsilon$ represent a gaussian random process with zero mean which is <u>spatially stationary</u>.

Ass. 5 The mean electron density must be the same throughout the scattering region affecting the exploring radio waves.

The last assumption is a corollary of assumption 4 for the ionosphere when $\Delta\epsilon/\epsilon$ is expressed in terms of $\Delta N/N$. Both

assumptions arise from the requirement that the conditions for the Wiener-Khintchin theorem, which plays a vital part in the theory, be satisfied.

A moments reflection will show that for applications to single scattering situations these assumptions require use of pencil beams illuminating small scattering volumes. For radar backscatter from auroral ionization a further requirement is sufficiently short pulse lengths and that the backscatter is received either from a single, well defined range or that echoes received over a range interval can be separated. The requirements of the theory are satisfied in the case of single, forward scattering of radiation from radio stars or satellites, but hardly for multiple scattering. Since radar beams tend to be wide and backscatter may be received from fairly large regions, while multiple scattering must be expected for radio star and satellite radiations traversing the auroral ionosphere, the theory needs to be improved, that is, the conditions 4 and 5 weakened, to provide an applicable theory. It is fortunate that such an improvement through weakened conditions is feasable so a realistic theory, suitable for applications, can be established in principle.

The approach is to introduce the concept of a <u>locally stationary</u> random process and establish a generalized Wiener-Khintchin relation which holds for this situation. The notion of a locally stationary random process has been defined and discussed by Silverman[32], who also gives the required generalization of the Wiener-Khintchin theorem. The heuristic equivalent of this approach in which the locally stationary random process in

a region of space is approximated by suitable stationary processes for sufficiently small subdivisions of the region, is justifiable and theoretically sound.

The reader who is familiar with the use of the concept of local thermodynamic equilibrium in the theory of radiative transfer (see Chandrasekhar[26]), will intuitively realize that the introduction of local stationarity puts the theory of multiple, forward scattering on a sound theoretical foundation. The quasi point source nature of radio stars and satellites ensures that the theory is satisfactory not only in principle but directly applicable to the observations.

For radar backscatter from auroral ionization the improvement appears to be mainly theoretical because a wide echo range together with the smoothing of the backscattered radiation by the antenna beam introduces interpretational problems.

10. Application of Theory to Radio Star Visibility Fades

10.1 Solar corona

The yearly June occultations of the radio star Taurus A by the solar corona represent a phenomenon closely related to the radio star visibility fades caused by the auroral ionosphere. Hewish[33] has interpreted the Tau A visibility reductions observed with the University of Cambridge radio interferometers. He suggests that the decrease of the recorded amplitude of a radio star, viewed through the outer corona, is produced by the angular spread caused by the coronal irregularities. Hewish states that the decrease could arise in two ways as follows.

(i) Thin layer scattering. Only a fraction of the incident energy is scattered, corresponding to $\tau < 1$ or rms phase deviations smaller than one radian, but the scale, ℓ, of the irregularities is such that the spread of the angular spectrum is considerably greater than the angle between the interference maxima of any of the interferometers in use, so that only the unscattered energy is recorded.

(ii) Thick layer scattering. Most of the energy is scattered, corresponding to $\tau > 1$ or rms phase deviations larger than one radian, but the spread of the angular spectrum is comparable with the angle between the interference maxima so that the recorded amplitude depends upon the spacing of the different interferometers.

The observations permitted Hewish to rule out hypothesis (i), while they were found to fit hypothesis (ii). He then applied Fejer's[7] theory of small-angle multiple scattering by isotropic irregularities to the observations. The essential formula is

$$P(\theta) \propto e^{-\pi^2 \ell^2 \theta^2 / \tau \lambda^2} \quad \text{for} \quad \tau > 1 \tag{129a}$$

with

$$\tau = \overline{(\Delta\epsilon/\epsilon)^2}\ \pi^{5/2}\ \ell z/\lambda^2 \tag{129b}$$

$$= (8.06 \times 10^{-5})^2 \overline{(\Delta N)^2}\ \pi^{5/2} \ell z / f^4 \lambda^2$$

From the required spread of the angular spectrum, a lower limit for ΔN and ℓ is defined by

$$(130) \qquad P(\theta) = e^{-1} \qquad \text{or} \qquad \theta^2 = \overline{(\Delta\epsilon/\epsilon)^2}\,\sqrt{\pi}\,(z/\ell)$$

For the solar corona the values of $\overline{(\Delta N)^2}$ and ℓ are not known. Therefore Hewish could only determine values for the quantity $\overline{(\Delta N)^2}/\ell$, and minimum values for ΔN and ℓ.

10.2 Auroral ionosphere

The interferometer observations of the Cassiopeia A visibility fades reported by Cornell University workers[34] on the frequencies 53 and 201.5 Mc/s show conclusively that multiple scattering in thick layers of the auroral ionosphere is responsible. The same is indicated by the frequency dependence of the 223 and 456 Mc/s visibility fades observed at College, Alaska. For the auroral ionosphere a more favorable situation exists than for the solar corona since we have fairly definite estimates for the value of $\overline{(\Delta N/N)^2}$ and N, at least for the auroral E layer, and know the approximate size of the F layer irregularities from radio star and satellite radio signal scintillations. It will be helpful to have also estimates of the approximate size of E layer irregularities under auroral conditions. Local observations of visual aurora indicate the horizontal dimensions given in the following table.

Table I.1

Horizontal Dimensions of Auroral Forms

Homogeneous arc	North-South extent	1 - 5 km
Rayed arc	North-South extent	200 - 1000 m
Coronal filament	Transverse extent	$\geq$ 200 m
Individual rays	Transverse extent	50 - 200 m

From this and the information in subsection 4, we may adopt the following irregularity dimensions for the initial analysis of the radio star visibility fades.

Table I.2

Irregularity Dimensions for Auroral Ionosphere

Ionospheric Layer	Transverse size x_T	Transverse scale T	Longitudinal size x_L	Longitudinal scale L	Layer Height
	m	m	km	km	km
F	600	165	3-4	0.8-1.1	300-600
E	150-300	40-85	$x_L > x_T$	L > T	110-130
			$x_L < x_T$	L < T	90-110

The Ithaca, New York, observations on 53 and 201.5 Mc/s together with selected, representative College, Alaska, observations on 223 and 456 Mc/s, provide data for a determination of the characteristic properties of the multiple scattering layers causing radio star visibility fades. The following tables give the pertinent equipment parameters and the observational data used.

Table I.3

Radio Interferometer Data

f Mc/s	λ m	x_λ	w rad.	w arc	w' rad.	w' arc
53	5.66	50	.0026	9.'8	.0100	34'
		35	.0037	12.6	.0143	49
		20	.0065	22.4	.0250	86
		5	.0260	89	.1000	344
201.5	1.49	190	.00068	2.35	.0026	9
223	1.35	68	.0019	6.7	.0073	25
456	0.66	139	.0009	3.2	.0036	12

Table I.4

Cas A Lower Transit Observations at Ithaca, N. Y.

Date 1960	53 Mc/s V	53 Mc/s x_λ	201.5 Mc/s V	201.5 Mc/s x_λ	K Index
Jan. 30	0.8	5	0.9	190	0
	0.4	20			
	0.2	35			
Feb. 4	0.5	5	0.65	190	3
	0.1	20			
	0.0	40			
Apr. 2	0.3	5	0.0	190	7
	0.15	15			
	0.0	25			

Table I.5

Selected Observations at College, Alaska

Date	Source	Az	223 Mc/s V	223 Mc/s min	456 Mc/s V	456 Mc/s min	K Index
1957 Dec. 30	Cyg A	4°	0.3	9	0.6	9	2
1959 Nov. 26	Cas A	202	0.1	7	0.7	16	2*

* Active aurora

The quantity V appearing in the two last tables is the visibility of the interference pattern defined as

$$(131) \qquad V = (I_{max} - I_{min})/(I_{max} + I_{min})$$

where I_{max} and I_{min} are the maximum and minimum intensities or amplitudes. The antenna separation measured in wavelengths is denoted by x_λ. The duration of the visibility fades observed at College is given in minutes.

The magnitude of the visibility fades observed at Ithaca, New York, show a simple dependence on the magnetic activity K-index which was measured at Canadian stations near the auroral zone. There is no clear relationship between the visibility fades observed at College, Alaska, and the College magnetic K-index. It is important to note that during lower transit of Cassiopeia A at Ithaca, New York, the line-of-sight to the radio

star crosses the auroral zone F layer. The 400 km height level is crossed in geomagnetic latitude 65°N which is within half a degree of the geomagnetic latitude for College (64.5°N). The College observations were selected to include both a lower and near upper transit case of a deep visibility fade. The latter occurred when an active auroral form crossed the line-of-sight to the radio star as described in detail in Section III.

Conditions for V = 0. The conditions that the radio star interference trace shall be reduced to zero visibility due to multiple scattering in a thick layer are the following:

(i) The directly transmitted component must be reduced to at least $I_o e^{-1}$; that is, the optical thickness, s, must equal or exceed unity.

(ii) The semi-angle of the scatter beam, θ, must equal (or exceed) the angular width, $2w'$, for which complete incoherence is attained:

$$\theta = 2w' = 1/x_\lambda \tag{132}$$

The latter condition implies that the angular size of the central, almost uniformly illuminated part of the diffracted radio star disk equals the angle between the interferometer lobes.

When these conditions are satisfied, the following relations obtain.

Number of scatterings:

$$p = (kT\theta)^2/2 = (3/2)(2\pi T/\sqrt{3})^2(1/\lambda^2 x_\lambda) \quad \text{Transverse case} \tag{133}$$

$$p = \tfrac{1}{2}(T^2\cos^2\gamma + L^2\sin^2\gamma)(k/x_\lambda)^2 \quad \text{Longitudinal case}$$

$$\doteq \tfrac{1}{2}(kL/x_\lambda)^2 \quad \text{for} \quad \gamma \doteq \pi/2$$

Minimum value for scale length (transverse case):

$$(134) \qquad T/\rho z \sec \chi \geq 1.5\times10^{5}(1/\lambda_N)^{4}\overline{(\Delta N/N)^2}$$

when $L = \rho T$.

Scattering coefficient (transverse case):

$$(135) \qquad \kappa(\chi) = \int \bar{\sigma}_F \sec \chi \, d\Omega$$

$$= (\pi/2)\overline{(\Delta\epsilon/\epsilon)^2}\,(\lambda T)^{-2} \sec \chi$$

with

$$(136) \qquad \bar{\sigma}_F = \overline{(\Delta\epsilon/\epsilon)^2}(\pi/\lambda^2)^2 \bar{P}(\theta)$$

$$= \overline{(\Delta N^2/N_o^2)}(\pi/\lambda^2)^2 \bar{P}(\theta)$$

$$(137) \qquad N_o = n_o f_{mc/s}^2 \text{ electrons/m}^3 , \quad n_o = 1.24\times10^{10}$$

Optical thickness:

$$(138) \qquad s \doteq p \gg 1 ,$$

$$s = \tau \sec \chi = \kappa(\chi) z = \kappa(0) z \sec \chi .$$

The Ithaca observations where during total fades the antenna spacings are decreased till full, or at least partial, visibility is regained are very useful in that they give information on the actual angular spread of the diffracted radiation. Evaluation of the scattering conditions from a partial visibility fade only, when the antenna separation cannot be increased to produce a total fade, presents some difficulties. It is possible to work out solutions by successive approximation procedures based on the complete analytical expressions (100) and (105), using as a

starting point the fact that the term for the directly transmitted component must be less than the recorded intensity. Thus the magnitude of the visibility sets a lower limit on the optical thickness of the scattering layer. At College total or very deep partial visibility fades are observed on 223 Mc/s, but usually only fairly shallow fades with visibilities in the range 0.9-0.5 at 456 Mc/s. In the following analysis the attention is concentrated on the total or very deep visibility fades observed at Ithaca on 53 and 201.5 Mc/s and at College on 223 Mc/s.

The scattering properties of the auroral ionosphere will now be estimated in terms of a two-layer model based on the following transverse irregularity dimensions.

F layer: x_T = 600 meters , T = 165 meters

E layer: x_T = 150-300 meters , T = 40-85 meters .

The results obtained by application of the formulas (133)-(138) to the individual observations listed in tables I.4 and I.5 are discussed below.

Ithaca, February 4, 1960

Number of scatterings in F layer: p = 10.5 for 53 Mc/s

Slant thickness: z sec X = 6 km

Vertical thickness (apparent): z = 1 km

The slant thickness is an estimate obtained by assuming that the average distance between the scattering irregularities is 600 meters, which is justified by the fact that the direction of incidence is almost normal to the direction of the magnetic field. The apparent vertical thickness of 1 km indicates that the layer is no thicker than the longitudinal dimension,

$x_L = 3.6L$. The actual vertical thickness will depend on the ratio $\rho = L/T$. We may conclude that the 53 Mc/s visibility fade is due to the large number of scatterings of the incident radiation along the slant path through the auroral F layer. When the activity level is low such fades will therefore be observable only near lower transit of Cassiopeia A for the sub-auroral zone station in question.

Ithaca, April 2, 1960

Number of scatterings in F layer: $p = 27$ for 53 Mc/s

$p = 6$ for 201.5 Mc/s

Slant thickness: $z \sec X = 16$ km for 53 Mc/s

At the time of this observation the magnetic activity was high ($K = 7$), and it might be expected that the auroral activity would spread to lower latitudes and a scattering E layer appear in the radiation path also. A model calculation was made to test this possibility but the observational data do not allow a two-layer interpretation in this instance.

College, December 30, 1957

The visibility fade occurred at lower transit of Cygnus A. The situation is very similar to that at Ithaca on February 4, 1960 except that the radiation path must necessarily also cross the auroral E layer. It could be argued that at the low elevation angle of the source, 15.5°, and the low activity level, $K = 2$, there would be no auroral F layer effect. But the College observations of radar backscatter from auroral ionization show that scattering irregularities are regularly present out to slant ranges of at least 1000-1200 km. Also, as mentioned, for

an auroral zone station the K-index value seems unrelated to the occurrence and magnitude of visibility fades. A model calculation based on F layer multiple scattering only indicates that this is a possible but not a reasonable solution. The resulting number of scatterings is $p = 43$. It was therefore assumed that the F layer conditions were similar to those found for the Ithaca 201.5 Mc/s observations on April 2, 1960, and a reasonable two-layer solution could be obtained on this basis as follows:

Number of scatterings in F layer: $p = 6$ for 223 Mc/s

Number of scatterings in E layer: $q = 8$ for 223 Mc/s

Slant F layer thickness: $z_1 \sec X = 3.6$ km

Slant E layer thickness: $z_2 \sec X = 2.4$ km

College, November 26, 1959

The two layer solution for this upper transit observation of Cassiopeia A is:

Number of F layer scatterings: $p = 6$ for 223 Mc/s

Number of E layer scatterings: $q = 16, 7, 4$ at 223 Mc/s

for transverse irregularity diameters of 300, 200, and 150 meters respectively. The last value, $q = 4$ using $x_T = 150$ meters, is the most reasonable although the condition $q \gg 1$ is not well satisfied. The vertical thickness of the scattering layers can only be deduced if assumptions about the ratio $\rho = L/T$ are introduced.

The results of the model calculations are summarized in the following table. The values for p, cos X and τ follow directly from the observations for the stated transverse

irregularity dimensions. It may be noted that the possible range of values for T which will give internally consistent results, is quite limited. The values for z and κ given in the tables depend on additional assumptions, and are not reliable.

Table I.6

Values for Multiple Scattering Layers

f	Layer	p,q	cos X	τ	z	κ	K	x_T	Activity
Mc/s					km			m	
53	F	10	0.173	1.7	1	1.7	3	600	Moderate
	F	27	0.173	4.7	3	13	7	600	Disturbed
201.5	F	6	0.173	1.05	3	3	7	600	Disturbed
223	F	6	0.29	1.75	1.5	2.6	2	600	Moderate
	E	8	0.29	2.3	0.7	1.6	2	300	Moderate
	E	4	1.0	4	3	12	2	150	Aurora
		7	1.0	7	3.5	30		200	
		16	1.0	16	5	80		300	
456	F & E		0.29	>0.2			2		Moderate
	F & E		1.0	>0.4			2		Aurora

The results indicate that the visibility fades of Cassiopeia A observed at the sub-auroral zone station Ithaca, New York, on 53 and 201.5 Mc/s during lower transit of the radio star are caused by multiple scattering in the auroral F layer under most activity conditions. The visibility fades of

Cassiopeia A and Cygnus A observed at the auroral zone station College, Alaska, on 223 and 456 Mc/s can in some cases be explained in terms of multiple scattering in the F layer only, but in general multiple scattering in both the auroral F and E layers appears to be the more reasonable explanation. In view of the differences in the geometrical factors both as regards the ionosphere and the radio interferometer systems, these statements do not contradict each other. The Ithaca data concern low elevation angle observations with interferometers which at 53 and 201.5 Mc/s have antenna separations of 50-5 and 190 wavelengths respectively. The College data involve visibility fades observed on 223 and 456 Mc/s at almost all azimuth and elevation angles with interferometers where the effective baselines vary in course of the day, and the maximum horizontal baseline at 223 Mc/s is only one-third of the 201.5 Mc/s antenna separation used at Ithaca. This suggests that if larger antenna spacings and preferably variable ones, had been available at College, many more visibility fades could have been recorded and studied more systematically. The actual number which may be observed with the present system is indicated by the following table for December 1957, a month which has been studied in detail.

Table I.7

Visibility Fades Observed at College December 1957

Source	223 Mc/s		456 Mc/s	
	Connected Events	Individual Events	Connected Events	Individual Events
Cas A	5	9	9	26
Cyg A	15	25	29	63
Total	20	34	38	89

For the purposes of this tabulation a visibility fade is counted as an individual event if the visibility is reduced to 0.5 for 3 minutes on 223 Mc/s and to 0.7 for 2 minutes on 456 Mc/s. The connected events are those where two or more individual fades occur within short time intervals of the order of minutes.

The table indicates a larger number of 456 than 223 Mc/s visibility fades but the selection criteria are somewhat biased in favor of the former. The larger number of fades recorded for Cyg A than for Cas A during December 1957, in spite of an equal division of the observing time between the two sources (alternatingly four days for each source), appears to have no particular significance when a longer period is considered. The total number of 223 Mc/s visibility fades for the five months December 1957, January and March-May 1958 is

Table I.8

223 Mc/s Fades for 5 Months

Source	Connected Events	Individual Events
Cas A	47	89
Cyg A	44	64

The strong correlation between the magnitude of the visibility fades and the magnetic K-index found for the Ithaca observations and the apparent lack of correlation for the College observations probably reflects the difference in mechanism. The results indicate that while formation of F layer scattering irregularities is magnetically controlled, other physical factors influence the formation of E layer irregularities and tend to mask the possible magnetic effects.

We concur in the view expressed by the Cornell University workers[34] that the radio star visibility fades cannot be explained in terms of a weak, single scattering process, or even by a few scatterings in an optically thin layer, because such processes will not reduce the directly transmitted radiation component sufficiently relative to the diffracted radiation. A strong scatter theory for the ionosphere, which to our knowledge has not been developed except in the case of scattering by critically dense or overdense ionization columns, could be invoked but appears implausible in view of the known properties of the auroral ionosphere and the observing frequencies used. The results of the analyses based on multiple scattering in one

or two, optically thick, layers could alternatively be expressed in terms of diffraction in an equivalent phase-changing screen, by use of the relations given at the end of 6.4 and in 7. The two-layer multiple scattering solution for the 223 Mc/s College observation on November 26, 1959 is equivalent to a diffraction pattern on the ground with structure of size 67.5 meters. In view of the equivalent rms phase deviations of the order of 3 indicated by the optical thickness, a structure of the order of 200 meters would be deduced for the diffracting screen, in good agreement with the results quoted in the discussion of the visibility fades in Section II by Little and Reid. The thick layer, multiple scattering solutions indicate that the finite size of the radio stars do not in the actual situations contribute significantly to the angular spread of the diffracted radiation although in principle this is a contributing factor.

11. Summary and Conclusions

The existing theory for weak, single scattering of radio waves by anisotropic ionospheric irregularities combines a Born approximation with a stochastic description of the properties of the medium. A critical examination has shown that the original form of the theory contains tacit assumptions introduced by the Wiener-Khintchin theorem which restrict its applicability. These restrictions can in principle be removed by introduction of the concept of a locally stationary random process and a suitable generalization of the Wiener-Khintchin relation. The resulting theory provides a satisfactory tool for analysis of scattering phenomena in the auroral ionosphere for the VHF and UHF radio

wave spectrum, excepting perhaps the lowest VHF decades.

The main problem remaining is the choice of an autocorrelation function which will give an adequate description of the electron density irregularities. The choice of a gaussian type autocorrelation function is upheld both for reasons of physical plausibility and mathematical convenience, although it is suggested that a modification accentuating small scale structure and discontinuities may be appropriate for analysis of back-scattered radiation. The final decision regarding the proper autocorrelation functions must be made on an empirical basis.

All experimental evidence indicates that the ionospheric electron density irregularities are elongated in the direction of the earth's magnetic field both in the F and the E layer. It is suggested that due to turbulence the E layer irregularities below 110 km may be flattened so their larger dimension is perpendicular to the magnetic lines of force. At the present stage the usual assumption of circular symmetry about the field line direction is a suitable working hypothesis, but the characteristics of main visual auroral forms show that one should be prepared to replace the prolate or oblate spheroid models with three-axial ellipsoid or other models whenever the observation so indicate.

A perusal of radio star and other radio investigations of the auroral ionosphere indicates that traversing radio transmissions may be subject to forward multiple scattering in regions or layers which are optically thick. It is suggested that multiple scattering layers may form in the E as well as the F

region. A physically correct interpretation of radio star and satellite radio signal transmission through the auroral ionosphere therefore requires a theory for multiple forward scattering by thick layers of anisotropic irregularities.

The astrophysical theory of radiative transfer in a scattering atmosphere can be invoked, and a solution ignoring backscatter, which is accurate to the first order or better, is obtained using the gaussian phase function or angular power spectrum derived from the theory of weak, single scattering in anisotropic irregularities. Convolution integrals are simple to evaluate for the gaussian type phase function, and the problem of multiple scattering in two layers having irregularities of different scale dimensions is solved in a first order, or better, approximation.

The diffraction effects of multiple scattering layers can be described in terms of equivalent, thin diffracting screens, but the direct relation to, and insight in, the physical process is lost.

The effect of finite source size on the diffracted radiation beam is investigated analytically. The conditions for regarding an extended source as a quasi point source are determined together with the correction procedures to be applied when the conditions are not fulfilled.

A two-layer model for forward multiple scattering of radio transmissions through the auroral ionosphere is used to explain visibility reductions of radio star signals observed on interferometers at Cornell University, Ithaca, New York, and the

University of Alaska, College, Alaska. The visibility reductions observed on two very-high frequencies during lower transits of Cassiopeia A from the 53.5°N geomagnetic latitude of Ithaca, N.Y., are explained in terms of auroral zone F layer multiple scattering. The visibility fades observed for Cassiopeia A and Cygnus A during upper and lower transits, and at other times, from the auroral zone location of College, Alaska, at a higher VHF and an ultra-high frequency, are best explained by multiple scattering in both the F and E layers. A difference in the dependence of visibility reductions on the magnetic K-index is noted for the two stations and related to a difference in the physical factors controlling irregularity formation in the F and E layer. Under the given experimental conditions, the angular spread of the diffracted radio star radiation emerging from the multiple scattering layers is insignificantly larger than the spread which would result for radiation from a point source.

The lack of movable antennas in the College experimental facilities has prevented systematic investigations of visibility fades so the quantitative data necessary for a complete analysis of the multiple scattering layers of ionization are not available. The estimates which could be derived from the existing limited Ithaca and College data show that experimental studies of radio stars with variable spacing interferometers provide a powerful tool for exploring the radio properties and physical characteristics of the auroral ionosphere. The most effective program of radio investigations would include coordinated investigations of the transmitted and forward scattered radiation from radio stars

and artificial satellites using spaced antenna, phase comparison and interferometer techniques, together with simultaneous radar investigations of the radiation backscattered from the auroral ionization in the E layer region traversed by the radio star or satellite signal.

References

1. Booker, H. G., A theory of scattering by nonisotropic irregularities with application to radar reflections from the aurora, Journ. Atmos. Terr. Phys., 8, 204, 1956.

2. Booker, H. G., The use of radio stars to study irregular refraction of radio waves in the ionosphere, Proc. I. R. E., 46, 298, 1958.

3. Ratcliffe, R. A., Some aspects of diffraction theory and their application to the ionosphere, Reports on Progress in Physics, XIX, 188, 1956.

4. Booker, H. G., and W. E. Gordon, A theory of radio scattering in the troposphere, Proc. I. R. E., 38, 401, 1950.

5. Silverman, R. A., On radio scattering by dielectric turbulence, Research Report No. EM-98, AFCRC-TN 56-797, AD 110138, Contract No. AF 19(604)-1717, Institute of Mathematical Sciences, New York University, September 1956.

6. Silverman, R. A., Fading of radio waves scattered by dielectric turbulence, Research Report No. EM-101 (No. 1) AFCRC-TN 57-379, AD 117081, Contract No. AF 19(604)-1717, Institute of Mathematical Sciences, New York University, January 1957.

7. Fejer, J. A., The diffraction of waves in passing through an irregular refracting medium, Proc. Roy. Soc. A, 220, 455, 1953.

8. Renau, J., Theory of spread F, Research Report EE 399, p. 2, Final Report, Contract No. DA36-039-sc-74903, School of Electrical Engineering, Cornell University, December 1958.

9. Pekeris, C. L., Note on scattering in an inhomogeneous medium, Phys. Rev., 71, 268, 1947.

10. Bailey, D. K., R. Bateman, L. V. Berkner, H. G. Booker, G. F. Montgomery, E. M. Purcell, W. W. Salisbury, A new kind of radio propagation at very high frequencies observable over long distances, Phys. Rev., 86, 141, 1952.

11. Spencer, M., The shape of irregularities in the upper atmosphere, Proc. Phys. Soc., 68B, 493, 1955.

12. Hewish, A., The diffraction of galactic radio waves as a method of investigating the irregular structure of the ionosphere, Proc. Roy, Soc., A, 214, 494, 1952.

13. Frihagen, J., and J. Trøim, A study of irregularities in the F region by means of transmissions from artificial satellites. NDRE Report No. 38, Technical Final Report, Contract AF 61(052)-344, Norwegian Defence Research Establishment, August 1961.

14. Bates, H. F., Direct HF backscatter from the F region. Journ. Geophys. Res., 65, 1993, 1960.

15. Nichols, B., Evidence of multiple scatter of radio-star signals at 53 Mc/sec, URSI Meeting, Washington, D. C., May 2-5,1960, Program p. 112.

16. Woodman, R. F., Irregular refraction of satellite signals observed at Ancon, Peru. Symposium of Space Research, Buenos Aires, Argentina, December 3, 1960; Report, NASA Satellite Tracking Station, Instituto Geofisico De Huancayo.

17. Cohen, R., and K. L. Bowles, On the nature of equatorial spread F, Journ. Geophys. Res., 66, 1081, 1961.

18. Bowles, K. L., R. Cohen, G. R. Ochs, and B. B. Basley, Radio echoes from field-aligned ionization above the magnetic equator and their resemblance to auroral echoes. Journ. Geophys. Res., 65, 1853, 1960.

19. Egan, R. D., Anisotropic field-aligned ionization irregularities in the ionosphere near the magnetic equator, Journ. Geophys. Res., 65, 2343, 1960.

20. Gallagher, P. B., Colloquium report at Stanford University (private communication).

21. Harang, L., "The Aurorae". Wiley, New York, 1951.

22. Størmer, C., "The Polar Aurora". Oxford University Press, 1955.

23. Howells, I. D., On the spectrum of electron density produced by turbulence in the ionosphere in the presence of a magnetic field, Journ. Geophys. Res., 64, 2198, 1959.

24. Rice, S. O., Mathematical analysis of random noise, Bell System Technical Journal, 23, 282, 1944; 24, 46, 1945.

25. Nichols, B., Drift motions of auroral ionization, Ph.D. Thesis, University of Alaska, 1957; Scientific Report No. 1, AFCRC-TN-58-123, AD145832, Contract No. AF 19(604)-1859, Geophysical Institute, University of Alaska, July 1957.

26. Chandrasekhar, S., "Radiative Transfer". Oxford University Press, 1950.

27. Van De Hulst, H. C., Scattering in a planetary atmosphere, Astrophys. Journ., 107, 220, 1948.

28. Hewish, A., The diffraction of radio waves in passing through a phase-changing ionosphere, Proc. Roy. Soc., A, 209, 81, 1951.

29. Wagner, L. S., Amplitude fluctuations in the Fresnel region of a phase-changing diffracting screen, Research Report RS 27, Contract No. AF 30(602)-2022, Center for Radiophysics and Space Research, Cornell University, August 1961.

30. Born, M., and E. Wolf, "Principles of Optics", Ch. X, Pergamon Press, New York 1959.

31. Shakeshaft, J. R., M. Ryle, J. E. Baldwin, B. Elsmore and J. H. Thomson, A survey of radio sources between declinations -38° and +83°, Memoirs Roy. Astron. Soc., LXVII, 97, 1955.

32. Silverman, R. A., Locally stationary random processes, Research Report No. MME-2, Contract No. DA 49-170-sc-2253, Institute of Mathematical Sciences, New York University, April 1957.

33. Hewish, A., The irregular structure of the outer regions of the solar corona, Proc. Roy. Soc., A, 228, 238, 1955.

34. Research Report RS 17, Atmospheric refraction of radio waves, Final Report, Contract No. AF 30(602)-2022, RADC-TR-60-148, Center for Radiophysics and Space Research, Cornell University, June 1960.

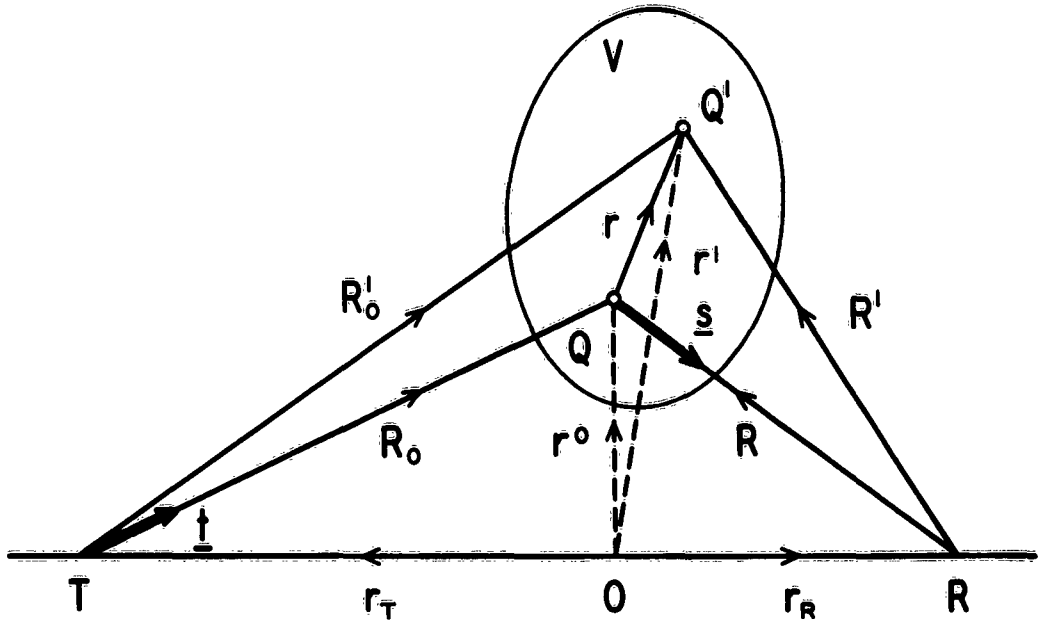

Fig. I.1 Geometry of scattering